This article has been accepted for publication in a future issue of this journal, but has not been fully edited. Content may change prior to final publication. Citation information: DOI 10.1109/TIA.2022.3144238, IEEE Transactions on Industry Applications

A Block-Coordinate-Descent Robust Approach to Incentive-Based Integrated Demand Response in Managing Multi-Energy Hubs with Must-Run Processes

Mehrdad Aghamohamadi, *Student Member, IEEE,* Amin Mahmoudi, *Senior Member, IEEE*, John K. Ward, *Member, IEEE,* Mohammed H. Haque, *Senior Member, IEEE*, João P. S. Catalão, *Senior Member, IEEE*

***Abstract*—This paper presents a new robust incentive-based integrated demand response (IDR) model for energy hub systems (EHSs). The considered incentive-based demand response (IBDR) schemes are interruptible/curtailable service (I/C) and capacity market program (CAP). The proposed IDR model integrates the arbitrage ability of EHS storages as well as energy conversion into the IDR model. The objective of the IDR optimization problem is to maximize/minimize the allocated incentives/penalties in targeted time periods by IBDR schemes, while supplying must-run processes with no interruption. Uncertainties of load and energy prices are considered through user-defined polyhedral uncertainty sets. A tri-level robust optimization (RO) is developed which includes a tri-level min-max-min problem. To solve the tri-level adaptive robust model, column-and-constraint generation (C&C) technique is employed by means of a decomposition methodology recasting the tri-level model into a single-level min problem and a bi-level max-min problem. Unlike previous RO models which solve the inner max-min problem by duality theory, a Block-coordinate-descent (BCD) methodology is used to solve the max-min problem by means of the first-order Taylor series in this study. The use of BCD technique instead of duality theory enables a recourse-based characterization of integer variables, such as EHS storage status, which was not applicable in previous models (due to use of duality theory). Moreover, Lagrange multipliers are eliminated as no duality is conducted. A post-event analysis is conducted to justify the long-term performance of the robust solutions and determine the optimal settings of the BCD robust approach. Results indicate that the IDR model significantly reduces the EHS input electricity in targeted time periods (four hours per day) by IBDR schemes and covers the required electricity with must-run processes by combined heat and power (CHP) unit, using natural gas. This implies a 2.13% reduction in the operation cost as incentives are obtained through IBDR schemes.**

***Index Terms*—Demand response, Energy hub, Multi-energy system, Robust optimization.**

NOMENCLATURE

A. Indices

f/j	Index of EHS input/output energy carriers.
i	Index of energy converter units.
k	Index of energy storage systems.
c/z	Index of outer/inner loop iterations.
t	Index of hour.

B. Parameters

A_{ft}	Allocated incentive to purchased energy reductions.
A_{ft}^{ex}	Extra incentive to extra energy reductions.
$\bar{C}_{ft}$	Nominal estimated energy price f in hour t.
$\hat{C}_{ft}^{dev+}$	Maximum positive deviation of energy price f in hour t.
$\hat{C}_{ft}^{dev-}$	Maximum negative deviation of energy price f in hour t.
d/m	Number of EHS input/output energy carriers.
E_{kt}^{up}/E_{kt}^{lo}	Maximum/minimum value of E_{kt}.
E_k^l	Energy loss for storage k.
Cl_{ft}	Contract level for IBDR schemes.
$\bar{L}_{jt}$	Nominal estimated value of load j in hour t.
$\hat{L}_{jt}^{dev+}$	Maximum positive deviation of load j in hour t.
$\hat{L}_{jt}^{dev-}$	Maximum negative deviation of load j in hour t.
n	Number of converter units.
N_X	Number of start-up variables in vector $\boldsymbol{X}$.
$N_{\tilde{U}}$	Number of uncertain parameters in vector $\widetilde{\boldsymbol{U}}$.
N_Y	Number of operation variables in vector $\boldsymbol{Y}$.
$\overline{P_{ft}}$	Expected purchased energy in targeted periods.
P_{ft}^{up}	Maximum value of P_{ft}.
$P_{it}^{\prime up}/P_{it}^{\prime lo}$	Maximum/minimum value of $P_{it}^{\prime}$.
Pen_{ft}	Allocated penalty for breaching IBDR contracts.
$Q_{kt}^{chg,up}/Q_{kt}^{chg,lo}$	Maximum/minimum value of Q_{kt}^{chg}.
$Q_{kt}^{dis,up}/Q_{kt}^{dis,lo}$	Maximum/minimum value of Q_{kt}^{dis}.
S_{jk}	Coupling factor between load j and storage k.
SUC_i	Start-up cost of converter unit i.
T	Number of hours of the scheduling horizon.
U_{it}^{ini}	Initial status of converter i in hour t (1:on, 0:off).
v_{fi}	Binary parameter which is 1 if i^{th} converter unit is supplied by f^{th} input energy and 0 otherwise.
η_{ji}^{con}	Converter's efficiency between input i and output j.
$\eta_k^{chg}/\eta_k^{dis}$	Charging/Discharging efficiency of storage k.
Ψ	Uncertainty budget.
ε	Convergence tolerance.

C. Sets

Ξ^C	Set of converter units.
Ξ^F	Set of EHS input energy carriers.
Ξ^I/Ξ^{II}	Set of "here-and-now"/"wait-and-see" variables.
Ξ^J/Ξ^K	Set of loads/storages.
Ξ^C/Ξ^z	Set of outer/inner loop iterations.
Ξ^T	Set of hours of the scheduling horizon.
Ξ^{UC}/Ξ^{UL}	Set of uncertain prices/loads.
Ξ^{US}/Ξ^S	Set of uncertainties/post-event scenarios.

D. Master Problem variables

C_{it}^{SU}	Start-up cost of converter unit i, in hour t.
U_{it}	Status of converter unit i in hour t (1:on, 0:off).
Λ_{I}	Value of master problem.

E. Sub-problem variables

Corresponding author: Mehrdad Aghamohamadi

M. Aghamohamadi and A. Mahmoudi are with the College of Science and Engineering, Flinders University, Adelaide, Australia (Email: mehrdad.aghamohamadi@flinders.edu.au, amaminmahmoudi@gmail.com).

John K Ward is with the Scientific and Industrial Research Organization, CSIRO Energy Center, NSW, Australia (Email: john.k.ward@csiro.au).

Mohammed H. Haque is with the University of South Australia, UniSA STEM, Adelaide, Australia (Email: mohammed.haque@unisa.edu.au).

João P. S. Catalão is with the Faculty of Engineering of the University of Porto and INESC TEC, Portugal (e-mail: catalao@fe.up.pt).

$\tilde{C}_{ft}$ Uncertain energy price f in hour t.
C_{ft}^{dev+} Positive deviation energy price f in hour t.
E_{kt} Energy level for storage k in hour t.
$\tilde{L}_{jt}$ Uncertain load j in hour t.
L_{jt}^{dev+} Positive deviation of load j in hour t.
$P_{ft}/\overline{P_{ft}}$ EHS purchased/forecast energy carrier f in hour t.
P_{ft}^{-}/P_{ft}^{+} EHS purchased energy carrier f in hour t, satisfying/breaching IBDR contracts.
P'_{it} Input energy to converter unit i in hour t.
PE Value of post-event cost.
$Q_{kt}^{dis}/Q_{kt}^{chg}$ Discharging/Charging rate of storage k in hour t.
$x_{kt}^{chg}/x_{kt}^{dis}$ Binary variable indicating charging/discharging status of storage k in hour t.
$\lambda_{ft}^{-}/\lambda_{ft}^{+}$ Binary variable for satisfying/breaching contract level.
$\Lambda_{\mathrm{II}}/\Lambda_{\mathrm{III}}$ Value of first/second-stage sub-problem.
λ,¥ Auxiliary continuous variables.

F. Vectors/Matrices

$\boldsymbol{A}, \boldsymbol{F}$ Coefficient matrices of objective function.
$\boldsymbol{B}, \boldsymbol{C}, \boldsymbol{E}, \boldsymbol{G}, \boldsymbol{H}/\boldsymbol{D}$ Coefficient/requirement vectors.
$\boldsymbol{P}/\boldsymbol{L}$ Vector of EHS input/output energy carriers.
$\boldsymbol{P'}$ Vector of EHS input energy to converter units.
$\boldsymbol{Q^{chg}}/\boldsymbol{Q^{dis}}$ Vector of storage charging/discharging rates.
$\boldsymbol{S}$ Storage coupling matrix.
$\overline{\boldsymbol{U}}/\boldsymbol{U^{dev+}}$ Vector of estimated/deviated uncertain parameters.
$\tilde{\boldsymbol{U}}$ Vector of uncertain parameters.
$\boldsymbol{V}/\boldsymbol{\eta}$ EHS configuration/conversion matrix.
$\boldsymbol{X}/\boldsymbol{Y}$ Vector of start-up/operation variables.
$\boldsymbol{X_c}$ Vector of obtained start-up variables in master problem to be send to sub-problem as fixed values.
$\boldsymbol{U^c}$ Vector of obtained worst-case realization of uncertain parameters in master problem.
$\boldsymbol{U^z}$ Vector of worst-case realization of uncertain parameters in second-stage sub-problem.

I. Introduction

A. Problem Description

DEMAND response (DR) is characterized through price-based (PBDR) and incentive-based (IBDR) schemes [1]. PBDR schemes are strong demand response signals that are mostly considered in every sector of energy distribution/delivery, i.e., industrial, residential, etc. [2]. However, IBDR schemes are generally developed through incentive/penalty terms according to which the end users agree to shift/curtail their demand. These schemes generally involve a provisional process interruption for customers as they need to reduce their input electricity [3] to optimize energy costs, directly affecting production procedures. Moreover, customers with must-run processes, i.e., non-curtailable loads, cannot participate in DR schemes properly as their input electricity is dependent on their process which cannot be interrupted [4]. In addition, the associated uncertainties with energy prices and demand poses a noticeable effect on optimal energy management of industrial customers especially during the targeted time periods by DR schemes. These uncertainties can change the operation of EHS such as the level of purchased energy from network and EHS facility operation. Hence, a proper integrated demand response modeling alongside a successful uncertainty characterization leads to higher benefits for multi-energy industrial customers with must-run processes.

B. Review on IDR and IBDR/PBDR applications

With the development of the energy hub system (EHS) [5-6], employed as an interface between different energy infrastructures and network participants, a new vision of DR has been introduced which is termed as "Integrated Demand Response" (IDR) [7-8]. IDR can easily make it possible for customers to actively participate in DR programs, even with non-curtailable loads, using energy conversion and storage facilities within EHS [9]. With IDR, it is possible to switch the consumed energy to other forms of energy at the EHS input ports, using converter elements such as CHP or micro turbines, or consume the stored energy by storage systems. As a result, the consumed energy at EHS input ports is levelized from the upstream network perspective, while the actual energy demand by EHS output ports are met with no interruption.

The arbitrage ability of EHS was employed in [10] to increase the benefits of a real world EHS through optimal interactions with upstream network and DR schemes. However, only PBDR schemes were considered in the model of [10]. Refs. [11] and [12] investigated the role of IDR in reducing the customers' payoffs, which is due to the ability of EHS in generating electricity from natural gas and battery systems in electricity peak periods where the electricity price reaches its maximum value. However, the models of [10-12] have only considered PBDR schemes in IDR. In fact, no IBDR schemes was included in the models in [10-12]. A similar PBDR approach was conducted in [13] to minimize the distributed smart energy hubs' payoffs considering only the electricity price. In [14], an optimization model was proposed to reduce energy costs of an EHS within IDR. However, the IDR model of [14] was also based on PBDR schemes and no IBDR scheme including incentive/penalty terms, was considered.

It is seen that, in many studies, IDR has been mostly modelled through PBDR schemes. This is because, PBDR schemes are strong and practical schemes that can motivate customers to participate in such a program and reduce their operation costs regarding upstream energy prices. However, IBDR schemes can also provide benefit recovery opportunities for energy system operators. In particular, IBDR schemes can direct EHS operators to switch the consumed electricity to other forms of energy to maximize their benefit and contribute in leveling the supply pattern from upstream network's perspective.

In [15] an IDR model was proposed for the application of both PBDR and IBDR schemes. However, the study of [15] does not consider the complex interactions among different energy carriers in EHS as it only considers the conventional single-energy demand response model of [15] for PBDR and IBDR schemes. In fact, the EHS responsiveness to IBDR and PBDR schemes are determined based on the DR model in [16], which was developed for single energy infrastructures. The obtained responsiveness patterns were then considered as operational constraints of the EHS. Therefore, the EHS responsiveness to DR schemes in [15] was not based on complex interactions among different energy carriers and/or the arbitrage ability of EHS through storage systems. The ability of EHS in supplying the required demand with multiple parallel paths allows the operator to participate in IBDR schemes flexibly, even with non-curtailable loads. For example, in the case of a considerable incentive allocation, the EHS operator switches the main electricity source to natural gas to cover the required electricity, using CHP or micro turbine. It can also consume the stored energy at the storage systems when directed.

TABLE I
ADVANTAGES OF THE PROPOSED MODEL COMPARED TO THE LITERATURE

Reference No.	Uncertainty modelling approach	Price-based IDR	Incentive-based IDR	Uncertainty consideration	Scenario generation required	Recourse-based IDR bids and storage operation
[9]	-	✓	×	No	-	×
[10]	-	✓	×	No	-	×
[11]	Stochastic programing	✓	×	Yes	Yes	×
[13]	-	✓	×	No	-	×
[14]	-	✓	✓	No		×
[17]	-	×	✓	No	-	×
[18]	Stochastic programing	×	×	Yes	Yes	×
[19]	Stochastic programing	×	×	Yes	Yes	×
[20]	Stochastic programing	✓	×	Yes	Yes	×
[22]	Dual-based RO	×	×	Yes	No	×
[23]	Dual-based RO	×	✓	Yes	No	×
[26]	Dual-based RO	×	×	Yes	No	×
[28]	-	✓	×	No	-	×
[29]	Stochastic programing	×	✓	Yes	Yes	×
Proposed model	BCD robust	✓	✓	Yes	No	✓

Therefore, the responsive load demand is curtailed from the network's perspective, while the actual energy requirements remain unchanged.

Considering the literature of IDR modeling, further studies are required to 1) characterize the incentive-based DR schemes within IDR concept, and 2) provide an integrated demand response model which employs EHS arbitrage abilities of EHS in performing IDR, resulting in a global optimum solution. Although, developing an incentive-based IDR model leads to lower/higher operational costs/benefits for EHSs, the uncertainties associated with EHS loads as well as energy price deviations at the upstream network can still pose significant effects on optimal operation of these systems [17].

C. Review On Uncertainty Modelling in EHS Operation

In the recent study of [18] an incentive-based IDR model was proposed, incorporating complex interactions among different energy carriers in EHS. Nevertheless, the employed IDR model was based on the conventional non-linear EHS model and no uncertainty characterization approach was conducted.

To obtain immunized solutions against uncertainties, the uncertainty sources in EHS operation were modeled through stochastic programing (SP), characterizing RES generation in [19] and demand uncertainty in [20]. SP was also employed in the IDR model of [21] for characterizing wind speed uncertainty. However, SP methods in [19-20] did not consider any IDR in their models. Although IDR was considered in [21], the conducted SP approach faces two main challenges including the lack of tractable methodology and the need of full distributional knowledge of uncertain parameters, which may not be easily available in practice [22].

Hence, the robust optimization (RO) technique as a tractable approach, eliminating the need of having full distributional knowledge of uncertain parameters, has been recently developed and applied to EHS operation in [23, 24]. However, the model in [23] is a single-stage RO with no recourse decisions to be made after uncertainty realizations, which may result in non-exact and non-realistic operational solutions. Moreover, no IDR was considered in [23]. Although, the model in [24] is a two-stage RO with recourse decisions, it has an extensive mathematical burden which is due to the simultaneous employment of decomposition methodology, duality theory, and big-M transformation technique when solving the optimization problem. In addition, no IDR was modeled in [24].

The use of duality theory limits the application area of RO in terms of characterizing mixed-integer models for recourse decisioning. This is because the dual of a mixed-integer model is generally weak, non-tractable and complicated [25]. Therefore, no binary variable can be modelled for recourse decisioning in RO. This issue becomes more important when binary variables, such as the storage charging/discharging status, need to be obtained after uncertainty realizations as recourse decisions. However, in the study of [24], converter start-up decisions and storage charging/discharging status are obtained before the uncertainty realization to ease the implementation of duality theory in the second-stage problem. In [26], a simplified model was considered in which duality theory was used to solve the energy hub operation.

Thus, a proper uncertainty characterization model is required to 1) overcome the non-tractability issues associated with scenario-based models such as SP, and 2) be able to characterize binary variables as recourse decisions after the uncertainty realization to achieve an optimal and realistic solution.

A brief of the conducted literature review has been given by Table I in which each study has been compared to the proposed BCD robust incentive-based IDR model in this paper. Accordingly, it is seen that the proposed model considers both IBDR and PBDR programs while being subject to uncertainties. It also does not require distributional knowledge of the generated uncertainty scenarios, compared to scenario-based and SP models. Moreover, due to the use of BCD technique, it provides recourse-based IDR bids and storage operation. In terms of mathematical burden of the proposed BCD robust model, following highlights are presented:

No duality is conducted in the proposed BCD robust model,

No linearization is required.

Therefore, compared to previous dual-based RO models, the proposed model in this study is subject to a less extensive mathematical burden.

In real-world cases, the arbitrage ability of storage operation provides the most important flexibility in the system when uncertainties arise. Therefore, determining storage operation after uncertainty realization in BCD robust model can reasonably improve the feasibility of the operation, compared to previous dual-based models.

As major advantages over previously reported methods, the proposed approach does not require duality-based cuts or linearization scheme. Moreover, some of the dual variables or Lagrange multipliers in dual-based RO models must be bounded through computationally expensive bounding parameter selection procedure which makes the model case-dependent. However, this issue is avoided in the proposed BCD robust model as no duality, and accordingly no dual variables or Lagrange multipliers are presented [30].

D. Motivations of this Study

Compared to the state-of-the-art, the main motivations of this study can be summarized as follows:

1) Current IDR studies have only modeled PBDR schemes, and no study has modeled the arbitrage ability of EHSs i.e., energy integration and storage, in performing IBDR schemes in the presence of uncertainties. Some studies have considered the uncertainty characterization approaches in their multi-energy management models, but no IBDR was modeled. Although PBDR schemes have a strong application in many energy systems today, it is time to go further and provide practical solutions for IBDR schemes in the IDR concept as incentive-based IDR has not been thoroughly investigated in this context.

2) In terms of uncertainty modeling, scenario-based and SP models are subject to non-tractability and non-accurate solutions, which is due to requiring a full distributional knowledge of uncertain parameters and a large number of scenarios (not applicable in practice). Therefore, further uncertainty modelling approaches are required to bypass the need of scenario generation.

3) Although RO has advantages compared to scenario-based and SP models, previous RO models in the literature fail to model binary variables such as EHS converters' on/off status and storage charging/discharging status as recourse decisions, which is due to the use of duality theory in solving the inner max-min problem.

E. Contributions

This paper is a continuation of an earlier work [26] in which duality theory was used to solve the energy hub operation. Accordingly, following innovative contributions are proposed to significantly extend the existing research and comprehensively meet all issues in previous studies:

Contribution 1: An incentive-based IDR model is proposed to characterize the allocated incentive/penalty terms of IBDR schemes in operation of EHSs with non-curtailable loads. The proposed model is conducted from the EHS's perspective, as an energy customer facing upstream IBDR schemes. Two commonly implemented IBDR schemes in the industrial sector, including interruptible-curtailable service (I/C) and capacity market program (CAP), are considered. The incentive/penalty terms and contract levels of I/C and CAP schemes are characterized to model the exact interactions between EHS and upstream IBDR schemes. Unlike a previous model [15], the proposed incentive-based IDR model in this paper is integrated into the EHS power flow constraints. In particular, it employs the arbitrage ability of storage systems as well as energy conversion throughout the EHS to maximize the incentive recovery and minimize penalty allocation.

Contribution 2: An adaptive robust optimization (ARO) approach is implemented to deal with the uncertainties of load and energy prices in operating EHSs. Uncertain parameters are characterized by bounded intervals in polyhedral uncertainty sets. The ARO model is a tri-level min-max-min problem which is not directly solvable. Therefore, a decomposition methodology is employed to recast the min-max-min ARO problem into two problems including a master problem and a sub-problem. A column-and-constraints (C&C) generation methodology is used to iteratively solve the decomposed problem through primal cutting planes. Several binary variables such as storage charging/discharging status as well as IC/CAP contract bids must be obtained after uncertainty realizations in the sub-problem to be able to compensate the effects of uncertain load/price as recourse decisions. Therefore, instead of using duality theory in solving the sub-problem, Block Coordinate Descent (BCD) method [27] is used in the proposed model (see the next contribution).

Contribution 3: In terms of solution methodology, BCD method [27] is used in the robust approach to iteratively solve the inner bi-level max-min sub-problem. This is implemented by means of Taylor series instead of transforming it into a single-level max problem by duality theory in conventional ARO models [28-29]. Therefore, the associated limitation in considering binary variables in the sub-problem is eliminated. In fact, mixed-integer models (even non-linear models) can be solved in the sub-problem through the proposed BCD robust model. As a result, uncertainty-dependent binary variables such as IDR bids and storage charging/discharging status can be obtained after uncertainty realization in the sub-problem as recourse decisions, resulting in more system flexibility in compensating the uncertainty effects such as load and price deviations. Moreover, the linearization of the dualized inner problem is avoided as the Lagrange multipliers are eliminated in this methodology. Thus, the case-sensitivity of the proposed incentive-based IDR model reduces as it does not reflect dual variables.

A post-event analysis has been presented against 25000 uncertainty realizations to validate the effectiveness of the obtained robust solutions against the uncertainties, compared to deterministic model.

II. Energy Hub Model

Fig. 1 is a general representation of an EHS as per the notations in the nomenclature. An EHS is an interface between energy suppliers at its input ports and energy requirements at output ports. These systems typically consume grid-bound energy carriers such as natural gas, electricity, and heat [31]. Energy inputs are directly consumed, converted to other forms of energy (i.e., using converter elements), and/or stored inside the system to be consumed in other operation time steps [32]. Since the input energy to EHS is consumed by several converters (such as natural gas that can be used in CHP, micro turbine, furnace, etc.), other variables named "dispatch factors" have to be considered in the model [32-34]. The idea of dispatch factors was first introduced by [35]. In this paper, the recent developed EHS model in [36] is employed in which the coupling matrix is replaced by two new matrices $\boldsymbol{V}$ and $\boldsymbol{\eta}$ alongside a new independent continuous variable P'_{it} which presents the input energy to each converter element. The relation between EHS input energy and the input energy to each converter is presented as (1a). Interested readers are referred to [36] for further information on the employed EHS model.

$$\underbrace{\begin{bmatrix} P_{1t} \\ \vdots \\ P_{ft} \\ \vdots \\ P_{dt} \end{bmatrix}}_{\boldsymbol{P}} = \underbrace{\begin{bmatrix} v_{11} & \dots & v_{1i} & \dots & v_{1n} \\ \vdots & \ddots & \vdots & & \vdots \\ v_{f1} & \dots & v_{fi} & \dots & v_{fn} \\ \vdots & & \vdots & \ddots & \vdots \\ v_{d1} & \dots & v_{di} & \dots & v_{dn} \end{bmatrix}}_{\boldsymbol{V}} \times \underbrace{\begin{bmatrix} P'_{1t} \\ \vdots \\ P'_{it} \\ \vdots \\ P'_{nt} \end{bmatrix}}_{\boldsymbol{P'}}; \tag{1a}$$

$$\text{where, } v_{fi} \in \{0,1\}, 1 \le i \le n, 1 \le f \le d, 1 \le t \le T; \tag{1b}$$

The relation between input energy to converters and EHs output loads is also provided by (1c).

This article has been accepted for publication in a future issue of this journal, but has not been fully edited. Content may change prior to final publication. Citation information: DOI 10.1109/TIA.2022.3144238, IEEE Transactions on Industry Applications

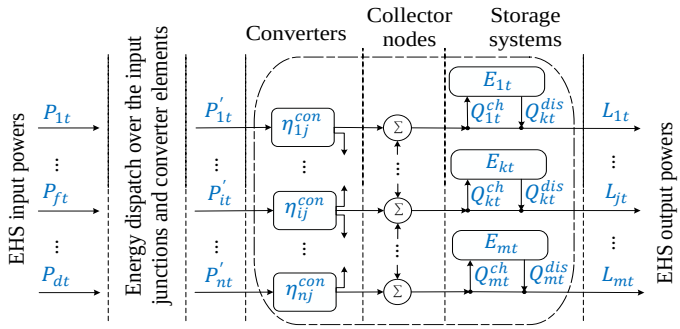

Fig. 1. General schematic representation of an EHS.

Each element of matrix $\boldsymbol{\eta}$ (η_{ji}^{con}) represents the efficiency of converter unit i converting its input energy to j^{th} EHS load.

$$\underbrace{\begin{bmatrix} L_{1t} \\ \vdots \\ L_{jt} \\ \vdots \\ L_{mt} \end{bmatrix}}_{\boldsymbol{L}} = \underbrace{\begin{bmatrix} \eta_{11}^{con} & \cdots & \eta_{1i}^{con} & \cdots & \eta_{1n}^{con} \\ \vdots & \ddots & \vdots & & \vdots \\ \eta_{j1}^{con} & \cdots & \eta_{ji}^{con} & \cdots & \eta_{jn}^{con} \\ \vdots & & \vdots & \ddots & \vdots \\ \eta_{m1}^{con} & \cdots & \eta_{mi}^{con} & \cdots & \eta_{mn}^{con} \end{bmatrix}}_{\boldsymbol{\eta}} \times \underbrace{\begin{bmatrix} P'_{1t} \\ \vdots \\ P'_{it} \\ \vdots \\ P'_{nt} \end{bmatrix}}_{\boldsymbol{P'}}; \quad (1c)$$

$$\text{where, } 0 \le \eta_{ji}^{con} \le 1, 1 \le i \le n, 1 \le j \le m, 1 \le t \le T; \quad (1d)$$

Accordingly, (1e) represents the energy flow between each EHS input energy and the input energy to converters.

$$P_{ft} = \sum\nolimits_{i \in \Xi^I} P'_{it} \cdot v_{fi}\,; \quad \forall f \in \Xi^F; \forall t \in \Xi^T \quad (1e)$$

Note that, storages can be placed in both inputs and outputs of the EHS. In fact, it is possible to transform storage power flows between inputs and outputs [40]. However, for modelling purposes in this paper (which is in line with previous studies such as [33], [35-36], and [40]), it is assumed that all the energy storages are at the output side. Accordingly, the linearized relationship between EHS inputs and outputs, considering converters and storage systems, would be as (1f) or its equivalent (1g).

$$\boldsymbol{L} = \boldsymbol{\eta} \cdot \boldsymbol{P'} - \boldsymbol{S} \cdot \boldsymbol{Q^{chg}} + \boldsymbol{S} \cdot \boldsymbol{Q^{dis}} \quad (1f)$$

$$\boldsymbol{L} = \boldsymbol{\eta} \cdot \boldsymbol{V^{-1}} \cdot \boldsymbol{P} - \boldsymbol{S} \cdot \boldsymbol{Q^{chg}} + \boldsymbol{S} \cdot \boldsymbol{Q^{dis}} \quad (1g)$$

Matrix $\boldsymbol{S}$ describes how changes of the storage energies affect the hub output flows. Each element of $\boldsymbol{S}$ illustrates the existence of energy trade between storage k and output load j ($S_{jk} \in \{0,1\}$). Therefore, in multi-period operation of the EHS, the following linear equation (1h) expresses the equality constraint between demand and supply which is the extended form of (1f).

$$\bar{L}_{jt} = \sum\nolimits_{i \in \Xi^I} \left(\eta_{ji}^{con} \cdot P'_{it}\right) + \sum\nolimits_{k \in \Xi^K} \left(S_{jk} \cdot Q_{kt}^{dis} - S_{jk} \cdot Q_{kt}^{chg}\right); \quad \forall j \in \Xi^J; \forall t \in \Xi^T \quad (1h)$$

III. Deterministic Incentive-based IDR Model

This paper has focused on I/C and CAP schemes which both include incentive and penalty terms. In these schemes, incentives usually consist of up-front reservation payments, and customers face penalties for failure to curtail when called upon to do so. Participants of I/C and CAP schemes should reduce their demand to an acceptable level. This level is known as contract level (Cl_{ft}) which is obtained as a part of the actual forecasted energy ($\overline{P_{ft}}$) in targeted time periods [18]. The values of incentive and penalty are allocated based on long-term contracts between the EHS operator and upstream network operator. However, the activation of DR service is broadcasted to the customers in different time frames such as daily or hourly notice of events [16]. The duration of notice is different from one customer to another and is based on the energy consumption of the customer and its flexibility in load shifting/curtailing.

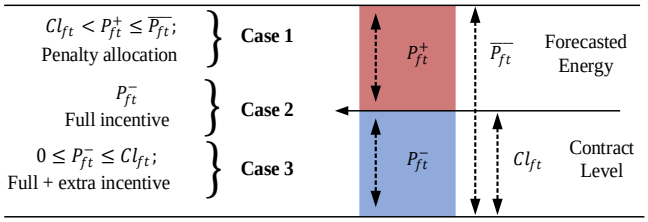

Fig. 2. Characteristics of IBDR contracts.

Some small-scale customers may be flexible enough and can participate in DR schemes by hourly notice. Some other large-scale industrial customers, however, require more time to participate in DR schemes [37]. In this study, it is assumed that the EHs operator is notified about the IBDR activation on a day ahead basis.

Fig. 2 represents IBDR contract's measures, as per the nomenclature of this paper. According to Fig. 2, participants can respond to the associated upstream IBDR schemes in three different ways [38], which are explained as follows:

***Case 1*:** Customer fails to respond to IBDR scheme and cannot fulfil the contract level i.e., the consumed energy is higher than the contract level. In this case, penalties are allocated to the uncurtailed energy. The consumed energy in this case is denoted as P_{ft}^{+}.

***Case 2*:** Customer fulfils the contract level in the IBDR scheme. The consumed energy is exactly equal to the contract level, and therefore, incentives are fully allocated to the curtailed energy. The consumed energy in this case is denoted by P_{ft}^{-}.

Case 3: Customer reduces its consumption more than the contract level in the IBDR scheme. In this situation, the curtailed energy is treated the same way as case 2, while the extra curtailed energy is rewarded with an additional rate of incentive.

In this section, a mixed integer linear incentive-based IDR model is presented for an EHS with non-curtailable loads, regarding possible EHS interaction with IBDR schemes, i.e., Cases 1-3. The model aims to a) optimally manage EHS facilities, including converters and storage systems, and b) maximize EHS benefits through IBDR schemes while mitigating actual energy consumptions by must-run processes at the EHS output.

The IDR model measures the EHS input electricity to gain maximum benefit and avoid any breach of contract in targeted time periods. Equation (2), represents the objective function and the associated constraints of the IDR model, considering the EHS operation and possible response to IBDR schemes by the EHS operator, i.e., Cases 1-3 presented by Fig. 2. The objective function (2a) encompasses five terms ($\mathbb{M}1, \ldots, \mathbb{M}5$).

The start-up cost of EHS converter units (i.e., CHP, heat exchanger, etc.) has been characterized in $\mathbb{M}1$, which is measured by the associated constraints of converter's on/off binary variables. The cost of EHS purchased energy carriers, regarding the hourly energy prices over the scheduling horizon, is presented through $\mathbb{M}2$. Binary variable λ_{ft}^{+} adds the third term (i.e., $\mathbb{M}3$) to the objective function (2a) if the EHS fails to fulfil the contract (Case 1 in Fig. 2). In fact, $\mathbb{M}3$ represents the penalty allocations pertaining to any possible breach of contract during the targeted time periods of IBDR schemes. In contrary, if the EHS fulfils the contract (Case 2 in Fig. 2), incentives would be allocated. This is modeled by binary variables λ_{ft}^{-} in $\mathbb{M}4$ which models the obtained incentives. The extra incentives due to higher values of purchased energy reductions (Case 3 in Fig. 2) are characterized by $\mathbb{M}5$. The considered incentives/penalties in the IDR model (2), i.e., Pen_{ft}, A_{ft}, A_{ft}^{ex}, are subject to change according to time and energy type. In fact, they are counted for all values of indices f and t. Therefore,

This article has been accepted for publication in a future issue of this journal, but has not been fully edited. Content may change prior to final publication. Citation information: DOI 10.1109/TIA.2022.3144238, IEEE Transactions on Industry Applications

they all can be fixed or time-varying in the operation of IDR (incentives and penalties for each energy type are vectors based on time).

Converters' start-up constraints are presented by (2b)-(2c). Note that, C_{it}^{SU} is a variables while SUC_i is a parameter reflecting the start-up cost of converter i (see nomenclature).

$$min \overbrace{\sum_{t\in\Xi^T}\sum_{i\in\Xi^C} C_{it}^{SU}}^{\mathbb{M}1} + \overbrace{\sum_{t\in\Xi^T}\sum_{f\in\Xi^F}\left(\bar{C}_{ft}.P_{ft}\right)}^{\mathbb{M}2} + \overbrace{\sum_{t\in\Xi^T}\sum_{f\in\Xi^F}\left(P_{ft}^{+}-\left(Cl_{ft}\cdot\lambda_{ft}^{+}\right)\right)\cdot Pen_{ft}}^{\mathbb{M}3} - \overbrace{\sum_{t\in\Xi^T}\sum_{f\in\Xi^F}\left(\left(\overline{P_{ft}}-Cl_{ft}\right)\cdot\lambda_{ft}^{-}\cdot A_{ft}\right)}^{\mathbb{M}4} - \overbrace{\sum_{t\in\Xi^T}\sum_{f\in\Xi^F}\left(\left(Cl_{ft}\cdot\lambda_{ft}^{-}-P_{ft}^{-}\right)\cdot A_{ft}^{ex}\right)}^{\mathbb{M}5}; \quad (2a)$$

$$C_{it}^{SU} \geq SUC_i\cdot\left(U_{i,(t=1)}-U_{it}^{ini}\right);\quad i\in\Xi^C;\forall t\in\Xi^T \quad (2b)$$

$$C_{it}^{SU} \geq SUC_i\cdot\left(U_{it}-U_{i,(t-1)}\right);\quad i\in\Xi^C;t\in\Xi^T|t>1 \quad (2c)$$

$$\lambda_{ft}^{+}+\lambda_{ft}^{-}\leq 1;\quad \forall f\in\Xi^F;\forall t\in\Xi^T \quad (2d)$$

$$P_{ft}=\sum_{i\in\Xi^I}P_{it}'\cdot v_{fi};\quad \forall f\in\Xi^F;\forall t\in\Xi^T \quad (2e)$$

$$P_{ft}^{-}+P_{ft}^{+}=P_{ft};\quad \forall f\in\Xi^F;\forall t\in\Xi^T \quad (2f)$$

$$Cl_{ft}\cdot\lambda_{ft}^{+}<P_{ft}^{+}\leq P_{ft}^{up}\cdot\lambda_{ft}^{+};\quad \forall f\in\Xi^F;\forall t\in\Xi^T \quad (2g)$$

$$0\leq P_{ft}^{-}\leq Cl_{ft}\cdot\lambda_{ft}^{-};\quad \forall f\in\Xi^F;\forall t\in\Xi^T \quad (2h)$$

$$\bar{L}_{jt}=\sum_{k\in\Xi^K}\left(S_{jk}\cdot\eta_k^{ch}\cdot Q_{kt}^{dis}-S_{jk}\cdot\frac{1}{\eta_k^{dis}}\cdot Q_{kt}^{chg}\right)+\sum_{i\in\Xi^I}\left(\eta_{ji}^{con}\cdot P_{it}'\right);\quad \forall j\in\Xi^J;\forall t\in\Xi^T \quad (2i)$$

$$P_{it}'^{lo}\cdot U_{it}\leq P_{it}'\leq P_{it}'^{up}\cdot U_{it};\quad i\in\Xi^C;\forall t\in\Xi^T \quad (2j)$$

$$E_{kt}=E_{k(t-1)}+\eta_k^{chg}\cdot Q_{kt}^{chg}-\frac{1}{\eta_k^{dis}}\cdot Q_{kt}^{dis}-E_k^{l}; \quad (2k)$$

$$\sum_{t\in\Xi^T}\left(\eta_k^{ch}\cdot Q_{kt}^{Chg}-\frac{1}{\eta_k^{dis}}\cdot Q_{kt}^{dis}\right)=T\cdot E_k^{l};\ \forall k\in\Xi^K; \quad (2l)$$

$$E_{kt}^{lo}\leq E_{kt}\leq E_{kt}^{up};\quad \forall k\in\Xi^K;\forall t\in\Xi^T \quad (2m)$$

$$Q_{kt}^{chg,lo}\cdot x_{kt}^{chg}\leq Q_{kt}^{chg}\leq Q_{kt}^{chg,up}\cdot x_{kt}^{chg};\forall k\in\Xi^K;\forall t\in\Xi^T \quad (2n)$$

$$Q_{kt}^{dis,lo}\cdot x_{kt}^{dis}\leq Q_{kt}^{dis}\leq Q_{kt}^{dis,up}\cdot x_{kt}^{dis};\ \forall k\in\Xi^K;\forall t\in\Xi^T \quad (2o)$$

$$x_{kt}^{chg}+x_{kt}^{dis}\leq 1;\quad \forall k\in\Xi^K;\forall t\in\Xi^T \quad (2p)$$

$$\forall x_{kt}^{ch},\forall x_{kt}^{dis},\forall U_{it},\forall\lambda_{ft}^{-},\forall\lambda_{ft}^{+}\in\{0,1\} \quad (2q)$$

$$\forall C_{it}^{SU}\forall P_{ft}^{-},\forall P_{ft}^{+},\forall P_{ft},\forall P_{it}',\forall Q_{kt}^{dis},\forall Q_{kt}^{Ch},\forall E_{kt}\in\mathbb{R}; \quad (2r)$$

The limitation constraint for λ_{ft}^{+} and λ_{ft}^{-} is presented as (2d) which explains that the EHS input electricity can either fulfil the contract or breach it at a time. The relation between EHS input energy carriers and input energy to converter units inside the EHS is described through (2e) and (2f). Note that, equations (2e) and (2f) are obtained based on the linearized form of EHS in (1). Constraints (2g) and (2h) limit the EHS input energies to their allowable ranges which are added to the objective function by means of binary variables λ_{ft}^{+} and λ_{ft}^{-}. If the EHS fails to fulfil the contract, its input energy is limited as (2g). Accordingly, $\mathbb{M}3$ would be included in the objective function while $\mathbb{M}4$ and $\mathbb{M}5$ are terminated with respect to (2d). Otherwise, (2h) is added as the EHS input energy limit, and $\mathbb{M}4$ and $\mathbb{M}5$ are added to (2a) instead of $\mathbb{M}3$. EHS energy balance constraint is expressed through (2i). Constraint (2j) limits the converters' input energy to their allowable ranges.

The energy balance of storage systems, considering charging, discharging, and standby modes is illustratively presented by Fig. 3. As it can be seen, the charging and discharging status, i.e., E^{cl} and E^{dl}, respectively, are subject to loss of energy, which is due to the storage efficiency in charging/discharging mode. Moreover, each storage is subject to steady-state mode losses, i.e., E^{l}. Accordingly, the dynamic energy balance for each storage k is expressed by (2k). Each storage at the final operational time period must have the same energy level as the first time period, which is known as end-coupling constraint and is expressed by (2l). If this equation is not considered in the model, the optimization still provides the optimal solutions. In fact, considering the end-coupling constraint can be similar to fixing the final value of storage level as its initial value. Ignoring this constraint does not affect the optimality of the solutions. The only difference is that the operation of the storage can be slightly different at the final period as it does not need to be charged again. The energy level, charging rate, and discharging rate for each storage are limited to their allowable ranges through (2m), (2n) and (2o), respectively. Constraint (2p) ensures that each storage operates in one mode only (charge, discharge, or out-of-use) at a time. Finally, the types of variables are specified in (2q) and (2r).

IV. Robust Approach to Solve the Incentive-Based IDR Model

A. Uncertainty Set Realization

The uncertainties associated with load and energy prices are considered by bounded intervals through polyhedral uncertainty sets as (3). The uncertain parameters $\tilde{L}_{jt}$ and $\tilde{C}_{ft}$ in (3) are allowed to deviate from their nominal estimated values $\bar{L}_{jt}$ and $\bar{C}_{ft}$ in positive and negative directions, which is shown by (3a) and (3b). The considered deviations are limited to their user-defined allowable ranges through constraints (3c) and (3d). The number of uncertain parameters pertaining to load and energy prices is determined by the uncertainty budget Ψ in (3e). If $\Psi=0$, no uncertain parameter can deviate from its estimated value, resulting in a deterministic model.

$$\Xi^{UL}=\left\{\tilde{L}_{jt}=\bar{L}_{jt}+L_{jt}^{dev+}-L_{jt}^{dev-};\quad \forall j\in\Xi^J;\forall t\in\Xi^T\right\} \quad (3a)$$

$$\Xi^{UC}=\left\{\tilde{C}_{ft}=\bar{C}_{ft}+C_{ft}^{dev+}-C_{ft}^{dev-};\quad \forall f\in\Xi^F;\forall t\in\Xi^T\right\} \quad (3b)$$

$$0\leq L_{jt}^{dev\pm}\leq\hat{L}_{jt}^{dev\pm};\quad \forall j\in\Xi^J;\forall t\in\Xi^T \quad (3c)$$

$$0\leq C_{ft}^{dev\pm}\leq\hat{C}_{ft}^{dev\pm};\quad \forall f\in\Xi^F;\forall t\in\Xi^T \quad (3d)$$

$$\Xi^{US}=\left\{\Xi^{UL}\cup\Xi^{UC},\sum_{t\in\Xi^T}\sum_{j\in\Omega^J}\left|\frac{L_{jt}^{dev+}}{\hat{L}_{jt}^{dev+}}+\frac{L_{jt}^{dev-}}{\hat{L}_{jt}^{dev-}}\right|+\sum_{t\in\Xi^T}\sum_{f\in\Omega^F}\left|\frac{C_{ft}^{dev+}}{\hat{C}_{ft}^{dev+}}+\frac{C_{ft}^{dev-}}{\hat{C}_{ft}^{dev-}}\right|\leq\Psi\right\}; \quad (3e)$$

By increasing the uncertainty budget, a greater number of uncertain parameters are allowed to deviate. The highest value for Ψ is equal to the total number of uncertain parameters allowing all uncertain parameters to deviate from their nominal estimates. Since robust optimization determines the solution based on the worst-case realization of uncertain parameters, it selects the maximum allowable value of deviation for each uncertain parameter. In fact, in the optimization $L_{jt}^{dev\pm}=\hat{L}_{jt}^{dev\pm}$ and $C_{ft}^{dev\pm}=\hat{C}_{ft}^{dev\pm}$.

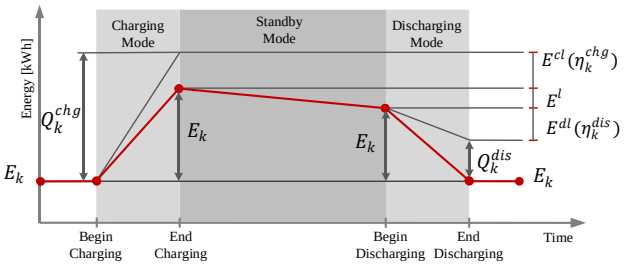

Fig. 3. Energy balance of storage systems.

Thus, equation (3e) illustrates the number of uncertain parameters deviating from their nominal values which is mathematically lower than Ψ. However, the optimization selects the exact value of Ψ as the uncertainty budget which is due to the conservativeness of robust optimization. Due to this reason, robust optimization has been considered as a conservative approach in uncertainty modelling, but more immunized against uncertainties. However, it is the post-event analysis which determines the optimal robust setting of the model. In fact, the post-event analysis examines different values of Ψ, $\hat{L}_{jt}^{dev\pm}$, and $\hat{C}_{ft}^{dev\pm}$ against trial scenarios to determine the most suitable robust settings. A more detailed explanation for this procedure is given in Section VI.C, where the post-event analysis is presented.

B. Proposed Adaptive Robust Model

Two main decisions are made in RO, including "here-and-now" decisions, which are obtained before any uncertainty realizations, and "wait-and-see" decisions, which are obtained after the realization of uncertain parameters [39]. As a result, when the uncertainties are realized, these “wait-and-see” recourse decisions can be adaptively made in response to uncertainty variation. This adaptive decision making capability brings an adaptive character into our robust model and makes it superior than a single-stage robust approach which has no “wait-and-see” recourse adaptivity. Due to this adaptive character, the proposed model has been called adaptive robust optimization.

In this study, the converters' start-up binary variables (i.e., U_{it}) are considered as "here-and-now" decisions, while other variables including EHS facilities' operation and input energy carriers are determined as "wait-and-see" decisions. The adaptive robust model is expressed through a tri-level min-max-min optimization problem as (4).

$$\min_{\boldsymbol{X}\in\Xi^{I}}\left(\boldsymbol{A'}\cdot\boldsymbol{X}+\max_{\widetilde{\boldsymbol{U}}\in\Xi^{US}}\min_{Y\in\Xi^{II}}\boldsymbol{F'},\boldsymbol{Y}\right) \tag{4a}$$

s.t.

$$\Xi^{I}=\{\boldsymbol{X}\in\{\boldsymbol{0},\boldsymbol{1}\}^{N_X}\mid \boldsymbol{CX}\geq\boldsymbol{D}\} \tag{4b}$$

$$\Xi^{II}=\left\{\boldsymbol{Y}\in\mathbb{R}^{N_Y}\mid \boldsymbol{E}(\boldsymbol{X},\boldsymbol{Y},\widetilde{\boldsymbol{U}})\geq 0\right\} \tag{4c}$$

$$\Xi^{US}=\left\{\widetilde{\boldsymbol{U}}\in\mathbb{R}^{N_{\tilde{U}}}\mid \widetilde{\boldsymbol{U}}=\overline{\boldsymbol{U}}+\boldsymbol{U}^{\boldsymbol{dev+}}\right\} \tag{4d}$$

In (4a), the outer min problem minimizes the term $\boldsymbol{A'}\cdot\boldsymbol{X}$ over "here-and-now" variables denoted by vector $\boldsymbol{X}$. This term represents $\mathbb{M}1$ in (2a) as the only dependent term on start-up variables to be obtained before any uncertainty realizations. The outer min problem is subject to constraint (4b) which represents the set of constraints (2b)-(2c) as the start-up characteristics. The inner min problem in (4a) minimizes the term $\boldsymbol{F'},\boldsymbol{Y}$ over "wait-and-see" variables, while the inner max problem maximizes it over the uncertain parameters.

The term $\boldsymbol{F'},\boldsymbol{Y}$ represents the set of the remaining terms in (2a) (i.e., $\mathbb{M}2$-$\mathbb{M}5$) which are dependent on "wait-and-see" variables, including EHS operation and energy flow variables. Therefore, the inner min problem is subject to constraints (2d)-(2p), represented by (4c), while the inner max problem is subject to uncertainty set realizations as (4d) which is the compact form of (3a)-(3b). A decomposition methodology is employed to decompose the tri-level min-max-min problem into a single-level min problem and a bi-level max-min problem by means of column-and-constraint generation technique [29]. The single-level min problem is called "master problem" and the bi-level max-min problem is called "sub-problem", hereafter. The extended version of master and sub-problem is given in the supplementary file.

C. Solution Methodology for the Tri-level Robust Model

The solution methodology includes two iterative loops namely the inner loop and the outer loop as depicted by Fig. 4. The compact mathematical formulations of master problem and sub-problem are given in Fig. 4, as per the notations in nomenclature. The outer loop in Fig. 4 is shown by red arrows while the inner loop is shown by green arrows. Each loop is described as follows:

1) Outer loop

The outer loop is responsible for transporting the obtained "here-and-now" variables in the master problem to the sub-problem (prior to uncertainty realizations), on one hand, and submitting primal cutting planes from sub-problem to master problem, on the other hand. The sub-problem is then solved given the obtained "here-and-now" variables to determine "wait-and-see" variables and the worst-case realization of uncertain parameters to be sent back to the master problem in the next iteration. Therefore, a complete set of primal cuts are added to the master problem in each iteration and "here-and-now" variables are updated to be sent to the sub-problem. This procedure iterates through the outer loop till the convergence criteria is met (values of master and sub-problem become sufficiently close) which terminates the outer loop and the robust solution is obtained.

2) Inner loop

Since the sub-problem is a bi-level max-min problem, it cannot be solved directly. In previous robust models such as [28-29], it was recast into a single-level max problem using duality theory which limits the application of RO. This is because no binary variables can be considered in the inner max-min problem as recourse decisions – dual of a mixed integer model is generally weak, non-tractable and complicated [25]. An example of these binary variables is the storage charging/discharging status that needs to be obtained after uncertainty realizations to compensate the shortage/surplus of energy due to uncertainties of load. Another example is the binary variables indicating the status of EHS in terms of responsiveness to the DR program which must be obtained after uncertainty realization to maximize the benefits of EHS. However, none of these are applicable through conventional dual-based robust models. This results in two unfavorable approaches (considering the literature), which are:

1) Removing the binary variables which is not applicable in some studies, like in this study where binary variables are allocated for failing or fulfilling IBDR contracts, i.e., λ_{ft}^{+}, λ_{ft}^{-}, and must be considered.

2) Characterizing binary recourse variables in the outer min problem (master problem) with no uncertainty characterization, while these variables are meant to be obtained after uncertainty realizations in the inner max-min sub-problem as recourse decisions. This results in non-optimal and non-realistic solutions. Therefore, in the proposed robust model in this paper, the BCD method is used to solve the sub-problem through an iterative methodology instead of transforming it to a single-level problem by duality theory. As a result, there is no limitation in considering binary variables in the inner max-min sub-problem.

This article has been accepted for publication in a future issue of this journal, but has not been fully edited. Content may change prior to final publication. Citation information: DOI 10.1109/TIA.2022.3144238, IEEE Transactions on Industry Applications

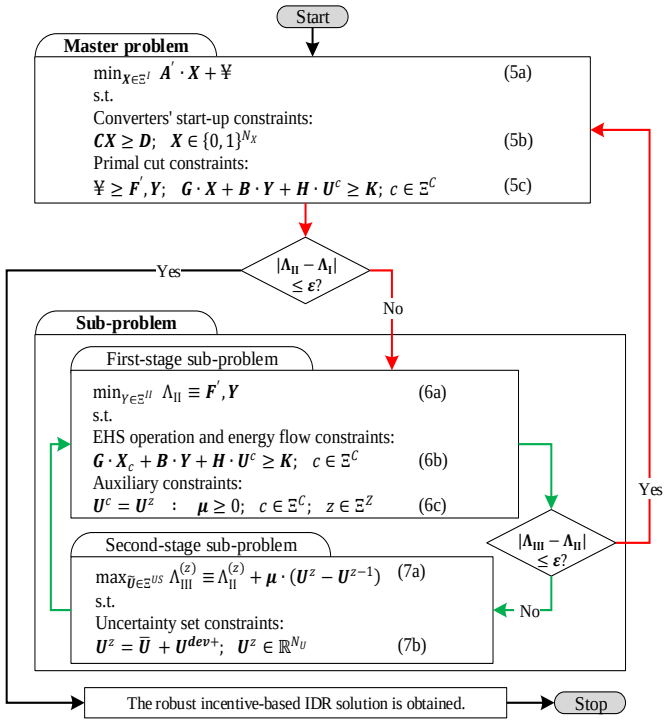

Fig. 4. Outline of the proposed two-stage BCD robust approach.

Therefore, the storage charging/discharging status variables as well as binary variables for failing or fulfilling IBDR contracts can be obtained after uncertainty realizations. This results in realistic and optimal solutions compared to those of the conventional dual-based robust models.

BCD technique was originally devised to deal with single-level problems. By extending the application of the BCD technique to solve the two-level max-min sub-problem (resulted from the C&C generation technique), it is possible to avoid duality theory in solving the sub-problem. Using the BCD methodology, the sub-problem is recast into a first-stage sub-problem (characterizing the inner min problem), and a second-stage sub-problem (characterizing the inner max problem). The second-stage sub-problem is built upon the first order Taylor series approximation of uncertain parameters in the first-stage sub-problem. The first-stage sub-problem determines the "wait-and-see" variables considering the worst-case realization of uncertain parameters obtained in the second-stage sub-problem, considering the obtained "here-and-now" variables from the master problem. The second-stage sub-problem is then solved to update the worst-case realization of uncertain parameters, considering the obtained "wait-and-see" variables in the first-stage sub-problem. This iterative procedure is executed through the inner loop. Therefore, in each iteration of the outer loop, the inner loop is executed till it converges (the value of first and second-stage sub-problems become sufficiently close).

The extended form of the BCD robust model has been presented in the Appendix at the end of this paper.

V. Performance Evaluation

A. Data Set

Fig. 5 shows the case study. The associated characteristics of the EHS are also presented in Fig. 5. These characteristics are taken from [40]. All inputs and outputs are in per unit (p.u.) with the base value of 100 kW. Table II lists the allocated incentives, penalties, and energy prices associated with upstream electricity market.

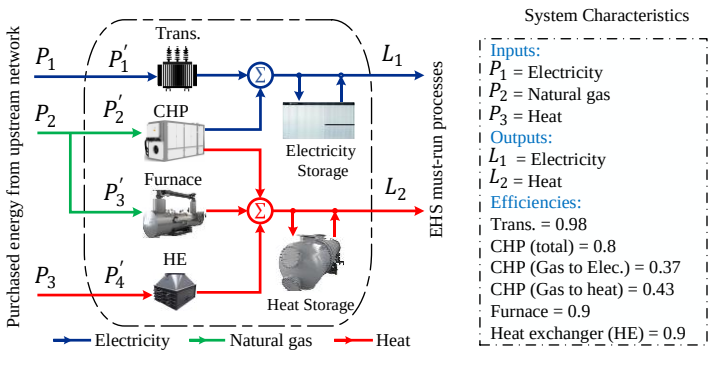

$$\eta = \begin{bmatrix} 1 & 0 \\ 1 & 1 \\ 0 & 1 \\ 0 & 1 \end{bmatrix} \quad V = \begin{bmatrix} 1 & 0 & 0 & 0 \\ 0 & 1 & 1 & 0 \\ 0 & 0 & 0 & 1 \end{bmatrix} \quad S = \begin{bmatrix} 1 & 0 \\ 0 & 1 \end{bmatrix}$$

Fig. 5. Studied EHS and its characteristics.

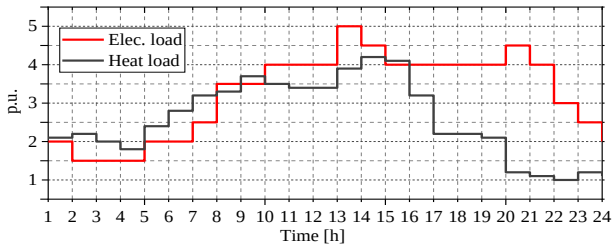

Fig. 6. Industrial electricity and heat energy consumptions

TABLE II
Scenarios and the Associated Characteristics [$/100kWh]

Elec. price			Incentive	Extra incentive	Penalty
Valley	Off-peak	Peak			
5.30	7.90	13.20	12.00	2.45	5.45

TABLE III
Input Parameters and Their Allowable Ranges

Parameter	Allowable range [p.u.]
EHS input Elec. / EHS input gas	$0 \leq P_{1t} \leq 5$ / $0 \leq P_{2t} \leq 5$
EHS input heat / Input gas to CHP	$0 \leq P_{3t} \leq 3$ / $0 \leq P'_{2t} \leq 3$
Input gas to furnace	$0 \leq P'_{3t} \leq 3$
Elec./Heat storage charge/discharge rate	$0.1 \leq Q_{kt}^{chg}/Q_{kt}^{dis} \leq 3.5/2.5$
Elec. / Heat storage energy level	$0.1 \leq E_{1t} \leq 4.0$ / $0.5 \leq E_{2t} \leq 3.0$
Heat storage energy level	$0.5 \leq E_{2t} \leq 3.0$

In TOU rate, hours 01-06, 07-14/21-24, and 15-20 pertain to valley, off-peak, and peak period, respectively. Note that, both the energy prices and the load demand at the EHS output are considered as uncertain parameters meaning they may deviate in hourly scale. This is due to the fact that, the operation simulations are conducted on an hourly basis. However, the scale of the simulation can be reduced to any other scale. This is in line with many previous studies such as [8], [14-16], [19-21], [23-24], [26], [28], [32], [35-36], and [40]. Input parameters and their allowable ranges are given by Table III. The value of incentives/penalties are taken from [38], while, TOU rates are taken from [41]. Targeted time periods for IBDR schemes are hours 17-20 with 2 p.u. contract level. Four cases are considered with different deviation range of uncertain parameters. These cases include Case 1, Case 2, Case 3, and Case 4 with 5%, 10%, 15%, and 20% deviation, respectively. Since, there are five uncertain parameters (i.e., three input energy prices and two load consumptions), there are $5 \times 24 = 120$ uncertain parameters during a 24-h scheduling horizon (i.e., $0 \leq \Psi \leq 120$). Fig. 6 shows the hourly electricity/heat consumption by EHS at output ports, which are uninterruptible. Load data has been taken from [42]. Therefore, the energy consumptions in Fig. 6 are not shiftable/curtailable but subject to uncertainty.

This article has been accepted for publication in a future issue of this journal, but has not been fully edited. Content may change prior to final publication. Citation information: DOI 10.1109/TIA.2022.3144238, IEEE Transactions on Industry Applications

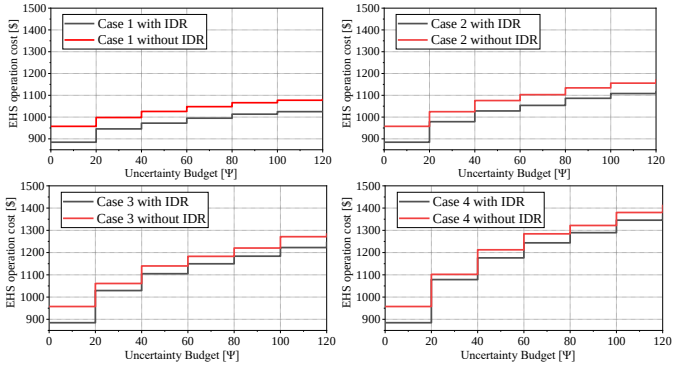

Fig. 7. EHS daily operation cost with and without the IDR model.

TABLE IV
TOTAL OPERATION COST FOR EACH CASE WITH 20-STEP SIZE Ψ

Ψ	Total operation cost [$/day]			
	Case 1	Case 2	Case 3	Case 4
0	884.73	884.73	884.73	884.73
20	945.75	978.85	1029.35	1078.53
40	972.07	1028.23	1104.91	1176.16
60	994.90	1053.60	1149.66	1243.71
80	1013.41	1086.21	1183.77	1289.52
100	1025.00	1108.01	1222.58	1345.72
120	1026.77	1119.54	**1248.38**	1372.11

Note that, any deviation in optimization parameters, such as input energy prices, does not affect the optimality of the solution. This is due to the fact that the optimization still reaches the global optima as the model is linear. Simulations have been conducted in GAMS software programing environment through GUROBI solver [43], on a computer with 8GB RAM and a Core-i7 CPU.

B. Robust Solutions

Table IV shows the EHS total operation cost for cases 1-4. It is observed that, $\Psi = 0$ stands as the deterministic representation of the proposed incentive-based IDR model, regardless of the deviation range of uncertain parameters. In fact, when $\Psi = 0$ no uncertain parameter can deviate from its estimate according to (3g).

As the uncertainty budget Ψ increments in Table IV, the total operation cost increases for all cases. This is because, increasing Ψ enlarges the size of the uncertainty set, i.e., a higher number of uncertain parameters can deviate from their nominal values, resulting in more robust operation at a higher expense. For a given value of $\Psi > 0$, the deviation of uncertain parameters in Case 4 > Case 3 > Case 2 > Case 1, which makes the worst-case realization of uncertainties even worst. Therefore, the operation cost of Case 4 > Case 3 > Case 2 > Case 1 for each value of Ψ. The computation time for all cases with different robust settings is between 3 and 4.5 seconds.

C. Validation of the Obtained Results

1) Comparison of the Solutions against PBDR scheme only

To illustrate the effectiveness of the proposed model, the studied EHS is operated in two scenarios. In the first scenario, only TOU pricing (which is a PBDR scheme) is considered, while in the second scenario both TOU and incentive-based IDR are considered. Therefore, the first scenario, i.e., TOU only, the objective function includes $\mathbb{M}1$, and $\mathbb{M}2$, while, the second scenario includes all terms $\mathbb{M}1$-$\mathbb{M}5$. The results of this operation are given by Fig. 7. As it is seen, the value of the objective function is lower in all cases 1-4 when considering incentive-based IDR in addition to TOU pricing. This is because the proposed model maximizes the obtained incentives while minimizing possible penalty allocations through IBDR schemes by optimally measuring input energies.

2) Validation of the Robust Solutions by Post-event Analysis

The obtained RO solutions become more immunized against uncertainties as the robustness level (value of Ψ, $\hat{L}_{jt}^{dev\pm}$, and $\hat{C}_{ft}^{dev\pm}$) increases. This feature is called "robustness worth" which is a result of high conservativeness, meaning that the prosumer will face minimum extra costs if uncertainties arise. However, this immunization comes at a higher expense which is called "robustness cost". This is shown in Table IV in which the value of objective function increases as the value of Ψ, $\hat{L}_{jt}^{dev\pm}$, and $\hat{C}_{ft}^{dev\pm}$ increase. Therefore, selecting a very high robustness level leads to over-conservative solutions, resulting in unnecessary robustness cost and impractical robustness worth, and vice versa.

To provide an optimal balance between robustness worth and cost, and to avoid over/under conservative RO solutions, a post-event analysis has been conducted in this study. According to this analysis, the obtained RO solutions for each robustness level (as indicated by Table IV) are examined against a sufficiently large number of uncertainty realizations, while the obtained operational solutions are fixed. The value of objective function is then normalized for all scenarios. The robust settings resulting in the lowest value of post-event value are considered as optimal robust settings of the model.

The energy shortage in each scenario has been modeled by additional free variables in the post-event analysis, to guarantee the feasibility of the solutions. This means, if a power shortage occurs, the additional free variables models the load shed. Therefore, the mixed-integer linear model (2) becomes a simple linear model, only characterizing power shortage. The mathematical model of post-event analysis is given as (8). Note that, only constraints associated with power shortage are considered in post-event model and other constraints are eliminated as they are fixed on the obtained robust solutions (they are constants and have no effect on the post-event value). The subscript ($_s$) in (8), indicates the associated variables in each trial scenario. The post-event value is obtained by (8a) in which the summation of the absolute value of power shortage, i.e., Y_{jts}^{sh}, for each trial scenario is normalized over the total number of trial scenarios. The only constraint being affected with power shortage is the energy balance constraint (2i) which is modified and presented by (8b).

$$PE = \sum_{s\in\Xi^S}\sum_{j\in\Xi^J}\sum_{t\in\Xi^T}\left(\frac{\left|Y_{jts}^{sh}\right|}{Total\ number\ of\ scenarios}\right) \quad (8a)$$

where;

$$\bar{L}_{jt} = \sum_{k\in\Xi^K}\left(S_{jk}\cdot\eta_k^{ch}\cdot Q_{kt}^{dis} - S_{jk}\cdot\frac{1}{\eta_k^{dis}}\cdot Q_{kt}^{chg}\right) + \sum_{i\in\Xi^I}\left(\eta_{ji}^{con}\cdot P_{it}'\right) + Y_{jt}^{sh};\quad \forall j\in\Xi^J;\forall t\in\Xi^T;\ \forall s\in\Xi^S; \quad (8b)$$

$$\forall Y_{jt}^{sh}\in\mathbb{R} \quad (8c)$$

The obtained results of the conducted post-event analysis are shown in Fig. 9. As can be seen, $\Psi = 0$ leads to a deterministic model resulting in higher post-event costs which illustrates that the deterministic solution is not immunized against load and energy price uncertainties. By increasing Ψ, the robustness of the proposed BCD robust model increases, which enlarges the size of polyhedral uncertainty set to cover more uncertainty realizations. The best performance of the ARO model is obtained as $1130.3 with 15% deviation of uncertain parameters (Case 3) and $\Psi = 120$.

This article has been accepted for publication in a future issue of this journal, but has not been fully edited. Content may change prior to final publication. Citation information: DOI 10.1109/TIA.2022.3144238, IEEE Transactions on Industry Applications

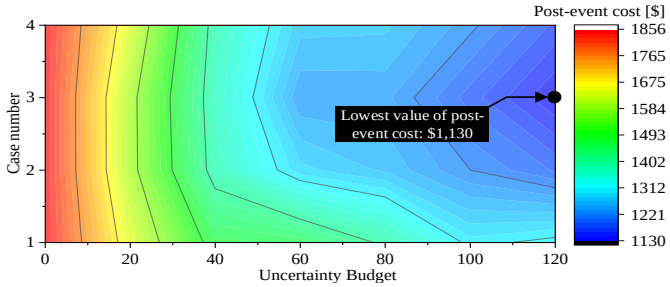

Fig. 8. Post-event cost of the EHS under different robust settings.

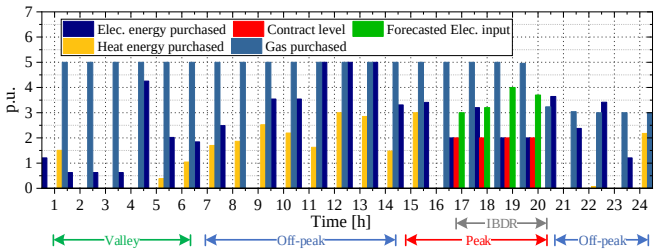

Fig. 9. EHS purchased energy carriers under the incentive-based IDR model.

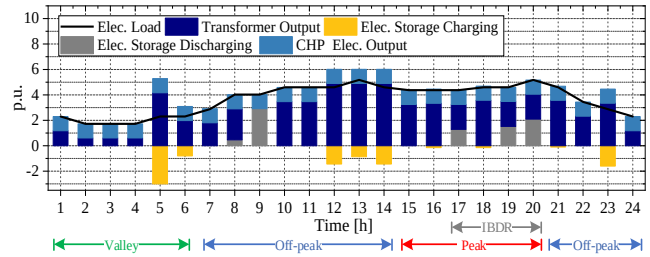

Fig. 10. Electric energy balance under the incentive-based IDR model.

These robust settings, therefore, result in the most practical, feasible, and economical performance of the proposed BCD robust model (see Fig. 8).

D. EHS Operational Solutions Based on the Obtained Optimal Robust Settings by Post-event Analysis

The following operational results are obtained under the optimum robust settings by post-event analysis in previous sub-section. Fig. 9 shows the EHS optimal purchased energies, including electricity, natural gas, and heat. It can be seen that, the EHS is more likely to consume input natural gas to generate electricity and heat (using CHP and furnace units) in most of the time. In targeted time periods by IBDR schemes i.e., hours 17 and 19-20, it has optimally purchased 2 p.u of electric energy, considering the 2 p.u contract level by IBDR schemes. Therefore, incentives have been fully allocated in these hours, according to $\mathbb{M}4$ in (2a). However, the input electricity has not been reduced in hour 18, which means the third term in (2a) (i.e., $\mathbb{M}3$) has been activated in this hour, allocating penalties to the unreduced purchased electricity.

Fig. 10 illustrates the energy balance and charging/discharging status for both heat and electricity storage systems. These solutions are obtained as recourse decisions due to the employment of BCD method in solving the max-min sub-problem. As it can be seen, the electricity storage has been considerably discharged in hours 17 and 19-20 to increase the EHS obtained incentives in targeted time periods by IBDR schemes. On the contrary, it has been reasonably charged in valley and off-peak hours such as hours 5-6 and 12-14 to contribute in the EHS optimal operation. The heat storage has been rationally charged in the early hours of the operation horizon and discharged during hours 14-16 to minimize the energy costs of the EHS while supplying non-curtailable loads.

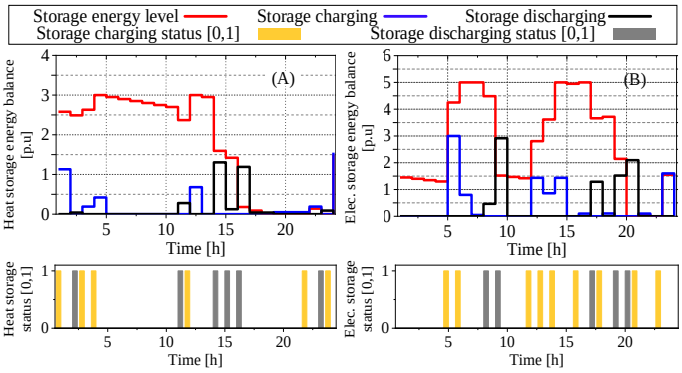

Fig. 11. Storage energy balance and charging/discharging status.

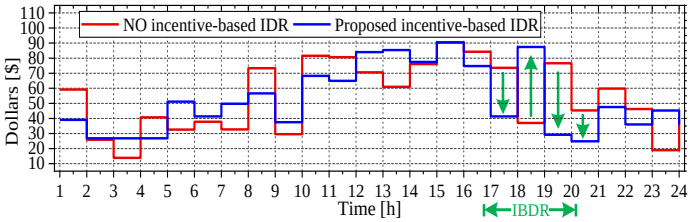

Fig. 12. Reduction of operation cost in targeted time periods by IBDR schemes.

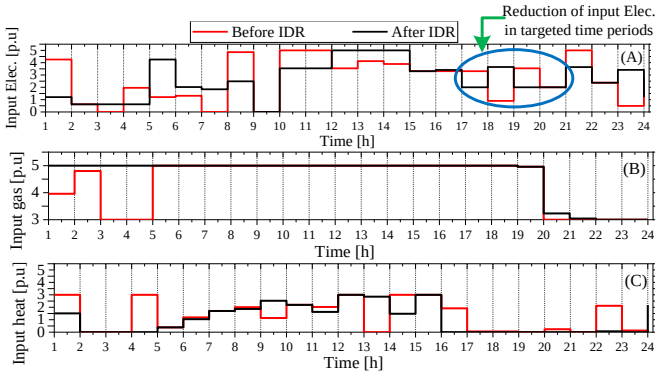

Fig. 13. Electricity, gas, and heat input before and after the proposed IDR model.

Note that, the required heat energy at the EHS output port in hours 15-24 (see Fig. 8), is covered by CHP as the input heat energy and the heat storage energy level is almost zero in these hours. The contribution of electricity storage system is shown in Fig. 11, indicating the variables associated with energy balance constraint (2i), including converters' output and charging/discharging of electricity storage. Note that, the EHS has supplied the consumed energy with no load shifting/curtailment at the demand side while participating in upstream IBDR schemes by optimal measuring of its input electricity. In fact, the actual energy consumption by non-curtailable loads at the EHS output port has remained unchanged while the input energy at the EHS input ports has been modified to satisfy upstream network IBDR schemes.

The hourly total operation cost of EHS, before and after the implementation of the proposed BCD robust IBDR model, is shown in Fig. 12. As it can be seen, the operation cost significantly reduces in hours 17 and 19-20, when using the proposed IDR model. This is because the EHS reasonably curtails the input electricity to obtain maximum benefits and avoid penalty allocations in these hours. It also consumes the stored electricity in the storage system to cover the required electricity in these hours (see Fig. 11). In hour 18, however, the operation cost under the proposed incentive-based IDR model increases as it purchases a higher value of input electricity, as shown in Fig. 9, resulting in a breach of contract and penalty allocations in this hour.

This article has been accepted for publication in a future issue of this journal, but has not been fully edited. Content may change prior to final publication. Citation information: DOI 10.1109/TIA.2022.3144238, IEEE Transactions on Industry Applications

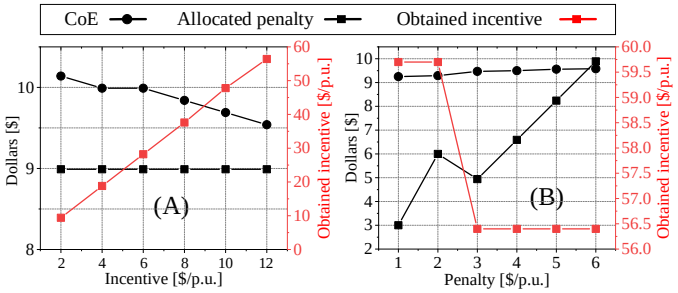

Fig. 14. Sensitivity analysis against different values of incentives/penalties

However, the total operation cost, when using the proposed incentive-based IDR model, is significantly lower than the total operation cost for the base scenario.

Modifications of input energy carriers by IDR are shown by Fig. 13 in which changes of the EHS input energy, before and after implementing the proposed BCD robust IDR model, are given. As it is seen, the electricity purchasing pattern by EHS has been modified, especially, in hours 17-20 which are the targeted time periods by IBDR schemes (see Fig. 13A). Moreover, it is seen that the modifications of input electricity purchasing pattern also affect other input energy carriers (see Fig. 13B, and 13C). This is because all input energy carriers are integrated in the EHS to supply EHS output load together (this shows the cross effects between different energy carriers when integrated in the IDR model).

E. Sensitivity Analysis

A sensitivity analysis has been conducted to investigate the sensitivity of the EHS total obtained benefits as well as the EHS cost of electricity (CoE) toward different incentives/penalties in IBDR contracts. Results are shown by Fig. 14. The EHS obtained incentives/penalties and CoE, during a 24-h operation, have been shown by Fig. 14A for different values of allocated incentive (from 2 $/p.u. to 12 $/p.u.) and a fixed value of penalty (5.4 $/p.u.) in IBDR contracts. As expected, the EHS total obtained incentive has increased while the allocated penalty has not changed at all. Accordingly, CoE has reduced from $10.14 to $9.54, illustrating the sensitivity of the proposed incentive-based IDR model to allocated incentives by IBDR schemes. The obtained results for different values of allocated penalties (from 1 $/p.u. to 6 $/p.u.) and a fixed value of incentive (12 $/p.u.) in IBDR contracts have been shown by Fig. 14B. As it is seen, the EHS total obtained incentive has reduced from $59.7 to $56.4 while the allocated penalty has increased. Therefore, the CoE would become greater as the value of penalty increases. As it is seen, the EHS benefit is highly sensitive to the allocated incentives and less sensitive to the penalty values in IBDR contract. This is because, the proposed model reduces the input electricity in targeted time periods by IBDR schemes. Therefore, there would be more incentive allocation than penalty allocation, resulting in higher sensitivity of CoE to incentives.

VI. Conclusion

A BCD robust incentive-based IDR model for multi-energy hub systems with non-curtailable loads was presented in this paper. The aim of the proposed IDR model was to consider incentive/penalty terms in IBDR contracts and provide a reasonable energy purchasing pattern for EHS under short-term operation uncertainties. The uncertainties of EHS of loads and energy prices were integrated into the model through a tri-level min-max-min robust optimization approach. BCD method was employed to solve the inner max-min problem, enabling the proposed IDR model to characterize binary variables after uncertainty realizations, which was not applicable in previous RO applications. This was because of eliminating the need of duality theory in solving the inner max-min problem.

Results showed that the IDR model reasonably reduces the EHS input electricity in targeted time periods (four hours per day) by IBDR schemes and covered the required electricity by CHP unit, using natural gas. Accordingly, no load curtailment was conducted at the EHS outputs, while the input energy is reduced reasonably to participate in upstream DR schemes. This resulted in a 2.13% reduction in the operation cost as incentives are obtained through IBDR schemes. The effectiveness of the incentive-based IDR model was illustrated by comparing the optimal results against a case with no incentive/penalty terms. The robust solutions were also compared to deterministic solutions in the post-event analysis. The value of objective function was considerably increased in the RO model, compared to the deterministic model. However, the RO solutions were more immunized against uncertainties as indicated by the post-event analysis. Accordingly, the post-event cost for the deterministic solutions was $1856, while this value was $1130 for RO solutions.

The proposed model can assist in the optimal operation of EHS facilities to efficiently participate in IBDR programs. The future work will focus on characterizing other types of IBDR schemes, such as emergency demand response.

Appendix: Extended Form of the BCD Robust Model

A. Master Problem

Master problem is solved to determine "here-and-now" decision variables including inverters' start-up solutions while being subject to star-up constraints only. Therefore, the objective function (9a) includes the term $\mathbb{M}1$ of the deterministic objective function (2a) and is subject to constraints (2b)-(2c) including start-up variables only, i.e., U_{it} and C_{it}^{SU}. Other operational constraints, therefore, are added as primal cuts in each iteration of the outer loop. The epigraph form of the master problem including primal cutting planes given by sub-problem, can be written as (9).

$$\text{Min } \Lambda_{\text{I}} \equiv \left(\overbrace{\sum_{t\in\Xi^T}\sum_{i\in\Xi^C} C_{it}^{SU}}^{\mathbb{M}1} \right) + ¥; \tag{9a}$$

s.t.

Converters' start-up constraints:

$$C_{it}^{SU} \geq SUC_i \cdot \left(U_{i,(t=1)} - U_{it}^{ini}\right); \quad i \in \Xi^C; \forall t \in \Xi^T \tag{9b}$$

$$C_{it}^{SU} \geq SUC_i \cdot \left(U_{it} - U_{i,(t-1)}\right); \quad i \in \Xi^C; t \in \Xi^T | t > 1 \tag{9c}$$

Primal cuts submitted from the sub-problem:

$$¥ \geq \left(\overbrace{\sum_{t\in\Xi^T}\sum_{f\in\Xi^F}\left(\tilde{C}_{ft}^{c}.P_{ftc}\right)}^{\mathbb{M}2} + \overbrace{\sum_{t\in\Xi^T}\sum_{f\in\Xi^F}\left(P_{ftc}^{+} - \left(Cl_{ft}\cdot\lambda_{ftc}^{+}\right)\right)\cdot Pen_{ft}}^{\mathbb{M}3} - \overbrace{\sum_{t\in\Xi^T}\sum_{f\in\Xi^F}\left(\left(\overline{P_{ftc}} - Cl_{ft}\right)\cdot\lambda_{ftc}^{-}\cdot A_{ft}\right)}^{\mathbb{M}4} - \overbrace{\sum_{t\in\Xi^T}\sum_{f\in\Xi^F}\left(\left(Cl_{ft}\cdot\lambda_{ftc}^{-} - P_{ftc}^{-}\right)\cdot A_{ft}^{ex}\right)}^{\mathbb{M}5} \right); \quad \forall c \in \Xi^C \tag{9d}$$

$$\lambda_{ftc}^{+} + \lambda_{ftc}^{-} \leq 1; \quad \forall f \in \Xi^F; \forall t \in \Xi^T; \forall c \in \Xi^C \tag{9e}$$

$$P_{ftc} = \sum_{i\in\Xi^I} P'_{itc}\cdot v_{fi}\,;\quad \forall f\in\Xi^F;\forall t\in\Xi^T;\forall c\in\Xi^C \tag{9f}$$

$$P^-_{ftc} + P^+_{ftc} = P_{ftc};\quad \forall f\in\Xi^F;\forall t\in\Xi^T;\forall c\in\Xi^C \tag{9g}$$

$$Cl_{ft}\cdot\lambda^+_{ftc} < P^+_{ftc} \le P^{up}_{ft}\cdot\lambda^+_{ftc};\forall f\in\Xi^F;\forall t\in\Xi^T;\forall c\in\Xi^C \tag{9h}$$

$$0 \le P^-_{ftc} \le Cl_{ft}\cdot\lambda^-_{ftc};\quad \forall f\in\Xi^F;\forall t\in\Xi^T;\forall c\in\Xi^C \tag{9i}$$

$$\tilde{L}^c_{jt} = \sum_{k\in\Xi^K}\left(S_{jk}\cdot\eta^{ch}_k\cdot Q^{dis}_{ktc} - S_{jk}\cdot\frac{1}{\eta^{dis}_k}\cdot Q^{chg}_{ktc}\right) + \sum_{i\in\Xi^I}\left(\eta^{con}_{ji}\cdot P'_{itc}\right);\quad \forall j\in\Xi^J;\forall t\in\Xi^T;\forall c\in\Xi^C \tag{9j}$$

$$P'^{lo}_{it}\cdot U_{itc} \le P'_{itc} \le P'^{up}_{it}\cdot U_{itc};\ \ i\in\Xi^C;\forall t\in\Xi^T;\forall c\in\Xi^C \tag{9k}$$

$$\sum_{t\in\Xi^T}\left(\eta^{ch}_k\cdot Q^{Chg}_{ktc} - \frac{1}{\eta^{dis}_k}\cdot Q^{dis}_{ktc}\right) = T\cdot E^l_k;\quad \forall k\in\Xi^K;\forall c\in\Xi^C \tag{9l}$$

$$E_{ktc} = E_{k(t-1)c} + \eta^{chg}_k\cdot Q^{chg}_{ktc} - \frac{1}{\eta^{dis}_k}\cdot Q^{dis}_{ktc} - E^l_k;\quad \forall k\in\Xi^K;\forall t\in\Xi^T;\forall c\in\Xi^C \tag{9m}$$

$$E^{lo}_{kt} \le E_{ktc} \le E^{up}_{kt};\quad \forall k\in\Xi^K;\forall t\in\Xi^T;\forall c\in\Xi^C \tag{9n}$$

$$Q^{chg,lo}_{kt}\cdot x^{chg}_{ktc} \le Q^{chg}_{ktc} \le Q^{chg,up}_{kt}\cdot x^{chg}_{ktc};\quad \forall k\in\Xi^K;\forall t\in\Xi^T;\forall c\in\Xi^C \tag{9o}$$

$$Q^{dis,lo}_{kt}\cdot x^{dis}_{ktc} \le Q^{dis}_{ktc} \le Q^{dis,up}_{kt}\cdot x^{dis}_{ktc};\quad \forall k\in\Xi^K;\forall t\in\Xi^T;\forall c\in\Xi^C \tag{9p}$$

$$x^{chg}_{ktc} + x^{dis}_{ktc} \le 1;\quad \forall k\in\Xi^K;\forall t\in\Xi^T;\forall c\in\Xi^C \tag{9q}$$

The objective function (9a) minimizes the converters' start-up costs by determining the start-up solutions as "here-and-now" decisions while being subject to start-up constraints (9b)-(9c). Constraints (9d)-(9q) represent the primal cuts submitted from the sub-problem. The subscript ($_c$) and the superscript (^{c}) in (9), indicate the associated "wait-and-see" variables and the fixed values of the uncertain parameters at iteration c of the column-and-constraint generation algorithm, respectively. Constraints (9e)-(9q) are equivalent to constraints (2d)-(2p). However, the forecast values of uncertain parameters in (2), i.e., $\bar{C}_{ft}$ and $\bar{L}_{jt}$, are replaced with the obtained worst-case realizations from the subproblem at iteration c, i.e., $\tilde{C}^c_{ft}$ and $\tilde{L}^c_{jt}$. The obtained start-up variables in master problem, i.e., U_{it} and C^{SU}_{it}, are then sent to the sub-problem as fixed values to determine both "wait-and-see" decision variables, i.e., EHS operation and energy flow variables, and the new worst-case realization of uncertain parameters.

B. Sub-problem

Sub-problem is solved to determine 1) optimal EHS operation and energy flow variables as "wait-and-see" decisions, and 2) the worst-case realization of uncertain parameters, given the fixed values of start-up variables obtained in master problem. In the conducted BCD methodology, the first-stage sub-problem is responsible for determining "wait-and-see" decision variables, while, the second-stage sub-problem determines the worst-case realization of uncertain parameters. In the following, both first and second-stage sub-problems are presented and discussed.

1) First-stage Sub-problem:

Since, the start-up variables are fixed on their obtained values by master problem, the term of the deterministic objective function (2a), as well as the start-up constraints (2b)-(2c) are not included in the first-stage sub-problem. Instead, it includes the term $\mathbb{M}2$-$\mathbb{M}5$ in (2a) and the associated EHS operation and energy flow constraints (2d)-(2p). The first-stage sub-problem is given by (10).

$$\begin{aligned}\text{Min } \Lambda_{\text{II}} \equiv\ & \overbrace{\sum_{t\in\Xi^T}\sum_{f\in\Xi^F}\left(\tilde{C}_{ft}.P_{ft}\right)}^{\mathbb{M}2} \\ & + \overbrace{\sum_{t\in\Xi^T}\sum_{f\in\Xi^F}\left(P^+_{ft} - \left(Cl_{ft}\cdot\lambda^+_{ft}\right)\right)\cdot Pen_{ft}}^{\mathbb{M}3} \\ & - \overbrace{\sum_{t\in\Xi^T}\sum_{f\in\Xi^F}\left(\left(\overline{P_{ft}} - Cl_{ft}\right)\cdot\lambda^-_{ft}\cdot A_{ft}\right)}^{\mathbb{M}4} \\ & - \overbrace{\sum_{t\in\Xi^T}\sum_{f\in\Xi^F}\left(\left(Cl_{ft}\cdot\lambda^-_{ft} - P^-_{ft}\right)\cdot A^{ex}_{ft}\right)}^{\mathbb{M}5};\end{aligned} \tag{10a}$$

s.t.

$$\lambda^+_{ft} + \lambda^-_{ft} \le 1;\quad \forall f\in\Xi^F;\forall t\in\Xi^T \tag{10b}$$

$$P_{ft} = \sum_{i\in\Xi^I} P'_{it}\cdot v_{fi}\,;\quad \forall f\in\Xi^F;\forall t\in\Xi^T \tag{10c}$$

$$P^-_{ft} + P^+_{ft} = P_{ft};\quad \forall f\in\Xi^F;\forall t\in\Xi^T \tag{10d}$$

$$Cl_{ft}\cdot\lambda^+_{ft} < P^+_{ft} \le P^{up}_{ft}\cdot\lambda^+_{ft};\quad \forall f\in\Xi^F;\forall t\in\Xi^T \tag{10e}$$

$$0 \le P^-_{ft} \le Cl_{ft}\cdot\lambda^-_{ft};\quad \forall f\in\Xi^F;\forall t\in\Xi^T \tag{10f}$$

$$\tilde{L}_{jt} = \sum_{k\in\Xi^K}\left(S_{jk}\cdot\eta^{ch}_k\cdot Q^{dis}_{kt} - S_{jk}\cdot\frac{1}{\eta^{dis}_k}\cdot Q^{chg}_{kt}\right) + \sum_{i\in\Xi^I}\left(\eta^{con}_{ji}\cdot P'_{it}\right);\quad \forall j\in\Xi^J;\forall t\in\Xi^T \tag{10g}$$

$$P'^{lo}_{it}\cdot U^c_{it} \le P'_{it} \le P'^{up}_{it}\cdot U^c_{it};\ \ i\in\Xi^C;\forall t\in\Xi^T \tag{10h}$$

$$\sum_{t\in\Xi^T}\left(\eta^{ch}_k\cdot Q^{Chg}_{kt} - \frac{1}{\eta^{dis}_k}\cdot Q^{dis}_{kt}\right) = T\cdot E^l_k;\ \forall k\in\Xi^K \tag{10i}$$

$$E_{kt} = E_{k(t-1)} + \eta^{chg}_k\cdot Q^{chg}_{kt} - \frac{1}{\eta^{dis}_k}\cdot Q^{dis}_{kt} - E^l_k;\quad \forall k\in\Xi^K;\forall t\in\Xi^T \tag{10j}$$

$$E^{lo}_{kt} \le E_{kt} \le E^{up}_{kt};\quad \forall k\in\Xi^K;\forall t\in\Xi^T \tag{10k}$$

$$Q^{chg,lo}_{kt}\cdot x^{chg}_{kt} \le Q^{chg}_{kt} \le Q^{chg,up}_{kt}\cdot x^{chg}_{kt};\forall k\in\Xi^K;\forall t\in\Xi^T \tag{10l}$$

$$Q^{dis,lo}_{kt}\cdot x^{dis}_{kt} \le Q^{dis}_{kt} \le Q^{dis,up}_{kt}\cdot x^{dis}_{kt};\ \forall k\in\Xi^K;\forall t\in\Xi^T \tag{10m}$$

$$x^{chg}_{kt} + x^{dis}_{kt} \le 1;\quad \forall k\in\Xi^K;\forall t\in\Xi^T \tag{10n}$$

$$\tilde{L}_{jt} = \tilde{L}^{(z)}_{jt}\ :\ \not{\beta}_{jt};\ \forall j\in\Xi^J;\ \forall t\in\Xi^T \tag{10o}$$

$$\tilde{C}_{ft} = \tilde{C}^{(z)}_{ft}\ :\ \not{\kappa}_{ft};\ \forall f\in\Xi^F;\ \forall t\in\Xi^T \tag{10p}$$

The objective function (10a) minimizes the energy costs while maximizing the EHS benefits through incentive/penalties as "wait-and-see" decisions to be obtained after uncertainty realizations. Constraints (10b)-(10p) are similar to those of the deterministic model but different in two ways, including 1) start-up variables, i.e., U_{it}, are fixed on the obtained "here-and-now" values in master problem at iteration c of the column-and-constraint generation methodology, i.e., U^c_{it}, and 2) the forecast values of uncertain parameters, i.e., $\bar{C}_{ft}$ and $\bar{L}_{jt}$, are fixed on the worst-case realization of uncertain parameters obtained by the second-stage sub-problem at iteration z of the BCD method, i.e., $\tilde{C}^{(z)}_{ft}$ and $\tilde{L}^{(z)}_{jt}$, by constraints (10o)-(10p).

Variables $\not{\beta}_{jt}$ and $\not{\kappa}_{ft}$ in (10o)-(10p) represent the sensitivity of the objective function (10a) toward uncertain parameters, including EHS demands and EHS input energy prices at each iteration z of the BCD method. These dual variables, indicated by vector $\boldsymbol{\mu}$ in (6c) in Fig. 5, are further employed to develop the second-stage sub-problem. As seen in (10), binary variables

including, $\lambda_{ft}^{+}, \lambda_{ft}^{-}, x_{kt}^{chg}$, and x_{kt}^{dis}, are characterized in the second-stage sub-problem to be obtained as "wait-and-see" variables indicating recourse decisions. This is due to the employment of BCD method which iteratively solves the bi-level max-min sub-problem through the inner loop (see Fig. 5) instead of transforming it to a single max problem by duality theory. Therefore, it is possible to determine the EHS status in fulfilling/failing IBDR contract as well as storage charging/discharging status after realizing the uncertainties in the sub-problem as "wait-and-see" decisions.

2) Second-stage Sub-problem:

The second-stage sub-problem is built upon the first order Taylor series approximation of the first-stage sub-problem over the uncertain parameters in the previous iteration of BCD method, i.e., $z-1$. Therefore, at iteration z of the BCD method, the second-stage sub-problem is cast as (11).

$$\text{Max}\ \Lambda_{\text{III}}^{(z)} \equiv \Lambda_{\text{II}}^{(z)} + \sum_{j\in\Xi^J}\sum_{t\in\Xi^T} \not{\kappa}_{jt}\left(\tilde{L}_{jt}^{(z)} - \tilde{L}_{jt}^{(z-1)}\right) + \sum_{f\in\Xi^F}\sum_{t\in\Xi^T} \not{\kappa}_{ft}\left(\tilde{C}_{ft}^{(z)} - \tilde{C}_{ft}^{(z-1)}\right) \quad (11a)$$

s.t.

(3a)-(3g) (11b)

The second-stage sub-problem determines the worst-case realization of uncertain parameters at each iteration z of the BCD method, by which the approximated objective function (11a) is maximized subject to the uncertainty sets presented by (11b).

REFERENCES

[1] D. Ellman and Y. Xiao, "Incentives to Manipulate Demand Response Baselines with Uncertain Event Schedules," in *IEEE Transactions on Smart Grid*, vol. 12, no. 2, pp. 1358-1369, March 2021.

[2] T. Khalili, H. G. Ganjehlou, A. Bidram, S. Nojavan and S. Asadi, "Financial Risk-Based Scheduling of Micro grids Accompanied by Surveying the Influence of the Demand Response Program," 2021 IEEE/IAS 57th Industrial and Commercial Power Systems Technical Conference (I&CPS), 2021, pp. 1-9, doi: 10.1109/ICPS51807.2021.9416627.

[3] M. Vahedipour-Dahraie, H. Rashidizadeh-Kermani, M. Shafie-Khah and J. P. S. Catalão, "Risk-Averse Optimal Energy and Reserve Scheduling for Virtual Power Plants Incorporating Demand Response Programs," in *IEEE Transactions on Smart Grid*, vol. 12, no. 2, pp. 1405-1415, March 2021, doi: 10.1109/TSG.2020.3026971.

[4] A. Jindal, M. Singh and N. Kumar, "Consumption-Aware Data Analytical Demand Response Scheme for Peak Load Reduction in Smart Grid," in *IEEE Transactions on Industrial Electronics*, vol. 65, no. 11, pp. 8993-9004, November 2018.

[5] S. Bahrami, M. Toulabi, S. Ranjbar, M. Moeini-Aghtaie and A. M. Ranjbar, "A Decentralized Energy Management Framework for Energy Hubs in Dynamic Pricing Markets," in *IEEE Transactions on Smart Grid*, vol. 9, no. 6, pp. 6780-6792, Nov. 2018, doi: 10.1109/TSG.2017.2723023.

[6] T. Liu, D. Zhang, H. Dai and T. Wu, "Intelligent Modeling and Optimization for Smart Energy Hub," in *IEEE Transactions on Industrial Electronics*, vol. 66, no. 12, pp. 9898-9908, December 2019.

[7] Y. Li, B. Wang, Z. Yang, J. Li and G. Li, "Optimal Scheduling of Integrated Demand Response-Enabled Smart Park Integrated Energy Systems in Uncertain Environment," in *IEEE Transactions on Industry Applications*, doi: 10.1109/TIA.2021.3106573.

[8] M. Geidl, et al, "The energy hub-A powerful concept for future energy systems," Third Annual Carnegie Mellon Conference on the Electricity Industry, 13-14 March 2007.

[9] Y. Li, H. Zhang, X. Liang and B. Huang, "Event-Triggered-Based Distributed Cooperative Energy Management for Multienergy Systems," in *IEEE Transactions on Industrial Informatics*, vol. 15, no. 4, pp. 2008-2022, April 2019.

[10] M. Kermani, E. Shirdare, A. Najafi, B. Adelmanesh, D. L. Carnì and L. Martirano, "Optimal Self-Scheduling of a Real Energy Hub Considering Local DG Units and Demand Response Under Uncertainties," in *IEEE Transactions on Industry Applications*, vol. 57, no. 4, pp. 3396-3405, July-Aug. 2021, doi: 10.1109/TIA.2021.3072022.

[11] P. Mancarella, G. Chicco, T. Capuder, "Arbitrage opportunities for distributed multi-energy systems in providing power system ancillary services," *Energy*, vol. 161, pp. 381-395, October 2018.

[12] V. Davatgaran, M. Saniei, S. S. Mortazavi "Smart distribution system management considering electrical and thermal demand response of energy hubs," *Energy*, vol. 169, pp. 38-49, February 2019.

[13] S. Bahrami and A. Sheikhi, "From Demand Response in Smart Grid Toward Integrated Demand Response in Smart Energy Hub," in *IEEE Transactions on Smart Grid*, vol. 7, no. 2, pp. 650-658, March 2016.

[14] F. Brahman, M. Honarmand, S. Jadid, "Optimal Electrical and Thermal Energy Management of a Residential Energy Hub, Integrating Demand response and Energy Storage System," *Energy and Buildings*, vol. 90, pp. 65-75, March 2015.

[15] M. Aghamohamadi, M. E. Hajiabadi, M. Samadi, "A novel approach to multi energy system operation in response to DR programs; an application to incentive-based and time-based schemes", *Energy*, Vol. 156, pp. 534-547, August 2018.

[16] H.A. Aalami, M. Parsa Moghaddam, G.R. Yousefi, "Demand response modeling considering Interruptible/Curtailable loads and capacity market programs," in *Applied Energy*, vol. 87, no. 1, pp. 243-250, January 2010.

[17] A. J. Conejo, M. Carrion, J. M. Morales, "Decision Making Under Uncertainty in Electricity Markets," Springer, New York, USA, 2010.

[18] S. Zheng et al., "Incentive-Based Integrated Demand Response for Multiple Energy Carriers Considering Behavioral Coupling Effect of Consumers," in *IEEE Transactions on Smart Grid*, vol. 11, no. 4, pp. 3231-3245, July 2020.

[19] A. Tavakoli, A. Karimi and M. Shafie-Khah, "Linearized Stochastic Optimization Framework for Day-Ahead Scheduling of a Biogas-Based Energy Hub Under Uncertainty," in *IEEE Access*, vol. 9, pp. 136045-136059, 2021, doi: 10.1109/ACCESS.2021.3116028.

[20] S. Moazeni, A. H. Miragha and B. Defourny, "A Risk-Averse Stochastic Dynamic Programming Approach to Energy Hub Optimal Dispatch," in *IEEE Transactions on Power Systems*, vol. 34, no. 3, pp. 2169-2178, May 2019.

[21] Y. Zhang, Y. He, M. Yan, C. Guo, Y. Ding, "Linearized Stochastic Scheduling of Interconnected Energy Hubs Considering Integrated Demand Response and Wind Uncertainty," *Energies*, vol. 11, No. 9, September 2018.

[22] X. Chen, Y. Zhang, "Uncertain linear programs: extended affinely adjustable robust counterparts," *Operation Research*, Vol. 57, pp. 1469-1482, November 2009.

[23] A. Mansour-Saatloo, M. Agabalaye-Rahvar, M. Mirzaei, B. M. Ivatloo, M. Abapour, K. Zare, "Robust scheduling of hydrogen based smart micro energy hub with integrated demand response," *Journal of Cleaner Production*, Vol. 267, September 2020.

[24] M. Aghamohamadi, N. Amjady, A. Attarha, "A linearized energy hub operation model at the presence of uncertainties: An adaptive robust solution approach," *International Transactions on Electrical Energy Systems*, vol. 30, no. 3, March 2020.

[25] M. Guzelsoy and T. K. Ralphs, "Duality for Mixed-Integer Linear Programs," *International Journal of Operations Research*, vol. 4, no. 3, pp. 118-137, January 2007.

[26] M. Aghamohamadi, A. Mahmoudi, J. K. Ward and M. H. Haque, "Two-stage Robust Management of PEV Parking Lots Coupled with Multi-energy Prosumers under Load and Energy Market Uncertainty," 2020 IEEE International Conference on Power Electronics, Drives and Energy Systems (PEDES), 2020, pp. 1-6, doi: 10.1109/PEDES49360.2020.9379335.

[27] A. J. Conejo, E. Castillo, R. M´ınguez, and R. Garc´ıa-Bertrand, "Decomposition Techniques in Mathematical Programming," *Engineering and Science Applications*. New York, NY, USA: Springer, 2006.

[28] M. Aghamohamadi, A. Mahmoudi, "From Bidding Strategy in Smart Grid Toward Integrated Bidding Strategy in Smart Multi-energy Systems, an Adaptive Robust Solution Approach," in *Energy*, vol. 183, pp. 75-91, September 2019.

[29] B. Zeng and L. Zhao, "Solving Two-Stage Robust Optimization Problems Using a Column-and-Constraint Generation Method," *Operation Research*, vol. 41, pp. 457-461, September 2013.

[30] R. Mínguez, R. García-Bertrand, J. M. Arroyo and N. Alguacil, "On the Solution of Large-Scale Robust Transmission Network Expansion Planning Under Uncertain Demand and Generation Capacity," in *IEEE Transactions on Power Systems*, vol. 33, no. 2, pp. 1242-1251, March 2018, doi: 10.1109/TPWRS.2017.2734562.

[31] M. Z. Oskouei, B. Mohammadi-Ivatloo, M. Abapour, M. Shafiee and A. Anvari-Moghaddam, "Strategic Operation of a Virtual Energy Hub With the Provision of Advanced Ancillary Services in Industrial Parks," in *IEEE Transactions on Sustainable Energy*, vol. 12, no. 4, pp. 2062-2073, Oct. 2021, doi: 10.1109/TSTE.2021.3079256.

[32] S. Zheng, Y. Sun, B. Li, B. Qi, X. Zhang, F. L, "Incentive-based integrated demand response for multiple energy carriers under complex uncertainties and double coupling effects," *Applied Energy*, vol. 283, February 2021.

[33] M. Geidl, G. Koeppel, P. Favre-Perrod, B. Klockl, G. Andersson and K. Frohlich, "Energy hubs for the future," in *IEEE Power and Energy Magazine*, vol. 5, no. 1, pp. 24-30, January 2007.

[34] D. Huo, C. Gu, K. Ma, W. Wei, Y. Xiang and S. Le Blond, "Chance-Constrained Optimization for Multienergy Hub Systems in a Smart City," in *IEEE Transactions on Industrial Electronics*, vol. 66, no. 2, pp. 1402-1412, February 2019.

[35] M. Geidl and G. Andersson, "Optimal Power Flow of Multiple Energy Carriers," in IEE*E Transactions on Power Systems*, vol. 22, no. 1, pp. 145-155, Feb. 2007, doi: 10.1109/TPWRS.2006.888988.

[36] M. Aghamohamadi, M. Samadi, I. Rahmati, "Energy generation cost in multi-energy systems; an application to anon-merchant energy hub in supplying price responsive loads," *Energy*, Volume 161, pp. 878-891, 2018.
[37] M. E. Honarmand, V. Hosseinnezhad, B. Hayes, M. Shafie-Khah and P. Siano, "An Overview of Demand Response: From its Origins to the Smart Energy Community," in *IEEE Access*, vol. 9, pp. 96851-96876, 2021, doi: 10.1109/ACCESS.2021.3094090.
[38] H.A. Aalami, M. Parsa Moghaddam, G.R. Yousefi, "Modeling and prioritizing demand response programs in power markets," *Electric Power Systems Research*, Volume 80, no. 4, Pages 426-435, April 2010.
[39] S. Wang and W. Pedrycz, "Data-Driven Adaptive Probabilistic Robust Optimization Using Information Granulation," in *IEEE Transactions on Cybernetics*, vol. 48, no. 2, pp. 450-462, Feb. 2018.
[40] M. Geidl, "Integrated modeling and optimization of multi-carrier energy systems," Eidgenssische Technische Hochschule Zurich, 2007.
[41] Ontario Energy Board. Approved prices and structures for electricity pricing pilots board file No.: EB-2016-0201. August 24, 2017.
[42] Available online: http://www.elia.be.com, [accessed 12 Dec. 2018].
[43] General Algebraic Modeling System, GAMS, https://www.gams.com/.

Mehrdad Aghamohamadi (Member, IEEE) received the B.Sc. degree in electrical engineering from Islamic Azad University, Sabzevar Branch, Sabzevar, Iran, in 2012, the M.Sc. degree in electrical power engineering from Hakim Sabzevari University, Sabzevar, Iran, in 2015, and the Ph.D. degree in electrical energy systems, from Flinders University, Adelaide, Australia, in 2021. Currently, he is an active energy market analyst in the industry. His research interests include sustainable and hybrid power and energy systems with applications in renewable energy generation, distribution, and its coordinated integration into energy sector. In particular, his research focuses on modeling and operation of multi energy systems and energy storage systems, uncertainty characterization, robust optimization, power market trades, electric vehicles integration, and demand response.

Amin Mahmoudi (S'11–M'13–SM'18) received the B.Sc. degree in Electrical Engineering from Shiraz University, Shiraz, Iran, in 2005, M.Sc. degree in Electrical Power Engineering from Amirkabir University of Technology, Tehran, Iran, in 2008, and the Ph.D. degree from the University of Malaya, Kuala Lumpur, Malaysia, in 2013. His main research interest is in areas where the electrical energy conversion plays a major role such as the electrical machines and drives as well as the renewable energy systems and hybrid power networks. It includes the transportation electrification in which the sustainable energy efficient solutions are realized by advanced electric motors, power electronics, energy management systems and controls for electrified powertrains, electric vehicles, etc. He has authored/co-authored over 130 papers in international journals and conferences. Dr. Mahmoudi currently works as a lecturer at Flinders University, Adelaide, Australia. He is a member of the Institution of Engineering and Technology (MIET) and a Chartered Engineer (CEng). He is also a member of the Engineers Australia (MIEAust) and Chartered Professional Engineer (CPEng).

João P. S. Catalão (Fellow, IEEE) received the M.Sc. degree from the Instituto Superior Técnico (IST), Lisbon, Portugal, in 2003, and the Ph.D. degree and Habilitation for Full Professor ("Agregação") from the University of Beira Interior (UBI), Covilha, Portugal, in 2007 and 2013, respectively. Currently, he is a Professor at the Faculty of Engineering of the University of Porto (FEUP), Porto, Portugal, and Research Coordinator at INESC TEC. He was the Primary Coordinator of the EU-funded FP7 project SiNGULAR ("Smart and Sustainable Insular Electricity Grids Under Large-Scale Renewable Integration"), a 5.2-million-euro project involving 11 industry partners. His research interests include power system operations and planning, power system economics and electricity markets, distributed renewable generation, demand response, smart grid, and multi-energy carriers

John K Ward (Member, IEEE) received the B.Sc. and Ph.D. degrees in Electrical Engineering from the University of Newcastle, Newcastle, Australia, in 1997 and 2002, respectively. He is the Research Director of the Energy Systems Research Program at the CSIRO and is responsible for driving the program's science direction and ensuring the program is developing a suite of science capability to meet future industry needs. His research is particularly focused on adding intelligence to the interaction of energy systems within the electricity distribution network.

Mohammed H. Haque (Senior Member, IEEE) received the B.Sc. and M.Sc. degrees in electrical engineering from the Bangladesh University of Engineering and Technology, Dhaka, Bangladesh, in 1980 and 1983, respectively, and the Ph.D. degree in electrical engineering from the King Fahd University of Petroleum and Minerals, Dhahran, Saudi Arabia, in 1988. During 1980–1983, he was with the Department of Electrical and Electronic Engineering, Bangladesh University of Engineering and Technology as a Lecturer. In 1984, he joined the Department of Electrical Engineering, King Fahd University of Petroleum and Minerals, as a Lecturer, and was promoted to an Assistant Professor in 1989 and an Associate Professor in 1993. During 1995–1997, he was with the School of Electrical Engineering, University of South Australia, Adelaide, SA, Australia, as a Senior Lecturer. He was also with The Flinders University of South Australia, Adelaide, SA, Australia, for one year. During 1999–2009, he was with the School of Electrical and Electronic Engineering, Nanyang Technological University, Singapore, as an Associate Professor. Since 2011, he has been with the University of South Australia. His research interest include power systems and renewable energy systems. He established the IEEE PES Chapter in South Australia Section in 2013. He was the recipient of the IEEE PES Chapter Outstanding Engineer Award in 2019. He is a Fellow of Engineers Australia.